Physiology and Pathophysiology of Microcirculation

18

Marc Thiriet

Contents

M. Thiriet (✉)
team INRIA-UPMC-CNRS REO, Laboratoire Jacques-Louis Lions, CNRS UMR 7598, Université Pierre et Marie Curie (Sorbonne Universités), Paris, France
e-mail: marc.thiriet@upmc.fr

P. Lanzer (ed.), *PanVascular Medicine*, DOI 10.1007/978-3-642-37078-6_24

Abstract

Microcirculation is the vascular compartments corresponding to vessels, the bore of which ranges from about five to a few hundred μm. Microcirculation possesses four main categories of conduits: arterioles, capillaries, venules, and terminal lymphatic vessels.

Microcirculatory driving pressure decreases from about 10.5–16 kPa (80–120 mmHg) in a supplying arteriole (bore 120 μm) to about 2.7 kPa (20 mmHg) in a draining venule (bore 120 μm).

Microcirculation regulates blood flow distribution within organs, nutrient delivery, transcapillary exchanges, and removal of cell wastes.

Glossary of Terms

Active hyperemia Local increase in blood flow rate caused by augmented activity of the perfused tissue.

Apparent viscosity (μ_{app}) or *effective viscosity* Viscosity of heterogeneous, non-Newtonian fluid that refers to the computation of the viscosity using the equations derived to calculate the viscosity of a homogeneous, Newtonian fluid (that remains invariant with changing shear rate at constant temperature and pressure). The viscosity is calculated from the Poiseuille law for a given flow rate and tube diameter. The apparent viscosity of blood, a concentrated suspension of mainly red blood capsules, decreases in microvessels (Fahraeus–Lindqvist effect), as the volume fraction close to the tube wall is reduced and the suspended particles do not contact the microvessel wall. This lubrification layer is less viscous than the suspension in the flow core. This phenomenon becomes stronger when the vascular caliber decreases relative to the particle size (i.e., in capillaries).

Autoregulation Maintenance of the local blood flow rate despite changes in driving pressure over a limited pressure range.

Fahraeus effect (local Ht < global Ht) Phenomenon that describes an attenuated average hematocrit (Ht; relative red blood capsule [RBC] concentration) in a steady blood flow in small straight tubes, the diameter of which is lower than 300 μm with respect to that in the upstream reservoir. This effect is generated in the concentration entry length of the tube, as red blood capsules move inside the central region of the tube lumen.

Fahraeus–Lindqvist effect (μ_b (d_h)) Effect that describes the apparent blood viscosity dependence on the microvessel hydraulic radius. This effect is observed when the characteristic dimension of a conduit approaches the size of seeded particles such as red blood capsules (7–8 μm) in suspension in the plasma (solvent), which is a tube diameter lower than 300 μm.

Glomerulus A capillary network between afferent and efferent arterioles surrounded by the Bowman's capsule that filters blood with a given glomerular filtration rate. A glomerulus and its Bowman's capsule constitute a renal corpuscle, the basic renal filtration unit.

Lymphatic capillary Conduit that carries interstitial materials back to the blood circulation. Interstitial materials enter lymphatic lumen through loose junctions between adjacent endotheliocytes. Lymphatic capillary localizes close to the blood capillary.

Metabolic response Adaptation of the local blood flow to the tissular metabolic rate. Any increase in cell activity elevates the temperature and liberates vasodilators (e.g., adenosine, bradykinin, histamine, and nitric oxide) that, together with a transient decrease in oxygen content and increase in carbon dioxide level, raise locally blood flow. The O_2 uptake is correlated with the local microvascular blood flow. The messenger ATP is released in microvessels by red blood capsules at a rate proportional to the decrease in oxygen saturation triggering a conducted response

that propagates upstream from the collecting venule through capillaries to the supplying arteriole to raise its caliber and, hence, local blood flow.

Metarteriole Short vessel that links an arteriole to a venule, hence shunting the capillary bed.

Myogenic response Adjustment of the vasomotor tone that adapts the vascular lumen size, hence the flow resistance, to keep the local blood flow constant, whatever the sensed transmural pressure in an autoregulation range, independently of endothelial influence.

Particle flow Flow characterized by a train of particles between which a solvent bolus is entrapped. In capillaries, red blood capsules surrounded by a lubricating plasma layer flow behind each other. When the particle concentration (that refers to the mass of particle per unit volume of solvent, whereas the particle density is the particle mass per unit volume of the particle) is high enough so that interactions between solvent and solute influence flow, only the average motion, and not individual particle movement, is explored. At a constant temperature, the quantities of interest for the solvent and particle are the pressure and the concentration, in addition to the velocity of both phases.

Plasma skimming Distributive process in branching sites of a capillary network associated with a core region with flowing red blood capsules and peripheral (near-wall) lubricating plasma layer. It is mainly observed in the kidney. Red blood capsules flow in larger capillaries, whereas only plasma flows in tiny capillaries (bore $\sim$5 μm).

Precapillary sphincter Muscular diaphragm at the capillary entrance close to the arteriole that regulates blood flow through the capillary.

Reactive hyperemia Increase in supplying blood flow rate associated with the vasodilation occurring after a sudden occlusion of the irrigating artery.

Introduction

Microcirculation is mainly aimed at maintaining an optimal perfusion of any organs according to its metabolic needs, that is, to its energetic demand by delivering a proper oxygen level.

Blood circulation ensures *homeostasis*, that is, the relative stability of internal conditions, a phenomenon described by the French physiologist C. Bernard in 1865, the word being later coined by the American physiologist W. B. Cannon. The internal conditions are monitored and regulated by a system of feedback controls to stabilize functioning of any biological components (cells, tissues, and organs). Corrective mechanisms are triggered that then reverses the original change toward the set point. The set level in fact oscillates constantly around the set point. Homeostasis then refers to a process of keeping the internal body environment in a quasi-steady state despite an unsteady external environment.

Any physiological quantity (e.g., blood pressure, volume, temperature, pH, and solute concentration) is enabled to vary only in a small range in normal conditions according to environmental stimuli, yet remaining relatively independent of its surrounding. A sensor detects changes, integrator processes this new condition, effectors transmit output signal, and a feedback corrects the situation.

The body's circulating fluids operate as control systems that protect the body's tissues from direct strong external influences by offering a stable internal environment. Internal processes operate to keep the conditions within tight limits to permit metabolic chemical reactions to proceed, whatever the scale, from the cell to the entire organism. Therefore, homeostasis enables enzymes to operate efficiently in fine-tuned conditions.

The central nervous system, liver, kidneys, lungs, and endocrine glands that interact via nerves and blood circulation participate in the maintenance of the body's homeostasis. The activity of the autonomic nervous and endocrine systems devoted to homeostasis is coordinated by the sensory hypothalamus that does not possess a

blood–brain barrier, hence receiving large molecules from blood, especially hormones. Neurons of the sensory circumventricular organs (CVO) such as subfornical organ (SFO) and organum vasculosum of the lamina terminalis (OVLT) devoid of blood–brain barrier and characterized by an extensive vasculature with fenestrated capillaries have receptors for many circulating hormones. Whereas the corrective response of the central nervous system is fast, hormone-controlled homeostatic mechanisms intervene with a significant time lag.

Blood composition is tightly controlled, that is, blood solute concentration is maintained in certain limits, especially that of required but toxic substances such as metallic element ions.

Glycemia, that is, the glucose concentration in blood, is strictly controlled (∼4 mmol/l, i.e., ∼82 mg/dl) although it varies between feeding and fasting, as chronic hyperglycemia exceeding 7 mmol/l (126 mg/dl) can produce organ damage. The pancreas has receptors that monitor the glycemia and endocrine cells in the islets of Langerhans that secrete antagonistic hormones; α and β cells release glucagon and insulin, respectively. The former supports glycogenolysis, hence elevating glycemia, and the latter glucose uptake and glycogenesis, thereby lowering glycemia.

Osmoregulation also controlled by the hypothalamus prevents loss or gain of water from cells. Osmosis, a type of diffusion, refers to the spontaneous displacement of solvent molecules through a semipermeable membrane (impermeable to large and polar molecules [ions, proteins, and polysaccharides] and permeable to nonpolar and hydrophobic molecules [lipids and gases, such as oxygen, carbon dioxide, and nitric oxide]) into a region of higher solute concentration to equalize the solute concentrations on both membrane sides. Osmosis yields the primary mechanism of water in- and outflux with respect to the cell cytosol. Water molecules can cross cell membrane through aquaporins, in addition to a direct passage through the lipid bilayer. Cell in a hypotonic or hypertonic medium gains or loses water, respectively. The osmotic pressure is the pressure required to maintain an equilibrium (absence of net solvent motion). Hypothalamic osmosreceptor cells that dilate or shrink whether plasma is dilute or has a high concentration of solutes ensure fluid balance. A decrease in water content detected by osmoreceptors stimulates the release of vasopressin, or antidiuretic hormone (ADH), from the pituitary gland. Vasopressin targets cells of the collecting ducts of the nephron, in which water molecules can only cross their membranes via aquaporins. It opens these pores, thereby increasing the permeability of the collecting duct wall. In addition to vasopressin, other hormones, such as aldosterone and angiotensin-2, control water reabsorption from glomerular filtrate in renal tubules. Kidneys achieve osmoregulation via 4 successive processes: (1) plasma filtration in the renal cortex from the glomerulus to the glomerular Bowman's capsule, (2) reabsorption in blood vessels that surround the convoluted tubule, (3) secretion of urine from collecting ducts to the renal medulla, and (4) excretion of urine stored in the bladder through the urethra.

Blood is a heat exchanger that regulates the body's temperature in diverse environment and climates to prevent cellular protein denaturation. The physical energy conservation principle must be applied. Internal corrective mechanisms can be coupled with behavioral processes to ensure an adequate nearly constant temperature of blood irrigating vital organs. Hot or cold weather initiates a voluntary response by dressing. The body's temperature is adjusted by the thermoregulatory center in the hypothalamus. The latter receives inputs from hypothalamic and cutaneous thermoreceptors that monitor the cerebral blood and external temperature. The hypothalamic thermostat then sends outputs to effectors to prime warming or cooling mechanisms. Heat is mainly produced by the liver, the body's chemical factory, and muscle contractions. In a hot environment, the body's cooling relies mainly on vasodilation of the cutaneous circulation and sweating. In a cold climate, the vasculature of the skin undergoes a vasoconstriction to limit heat loss (heat conservation), whereas the elevated metabolic rate upon stimulation by adrenal and thyroid glands, which secrete adrenaline and thyroxine, and shivering produces heat (thermogenesis). Smooth myocytes of cutaneous arterioles have thus a primary role in thermoregulation.

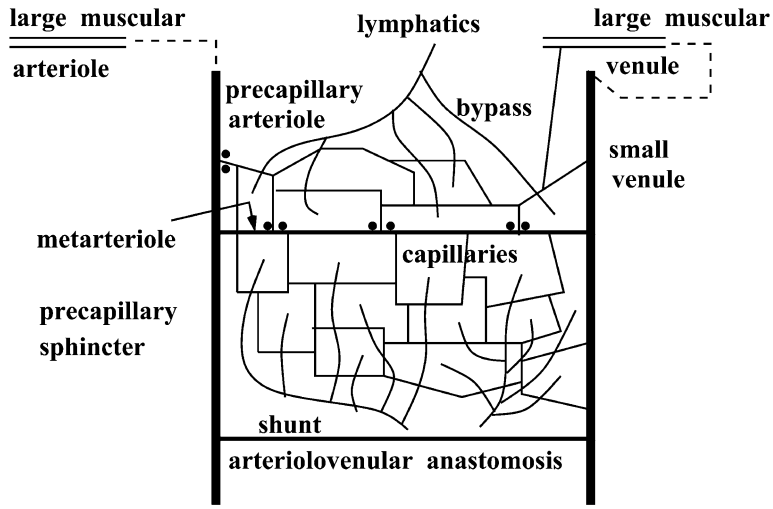

Fig. 1 Microcirculatory network with its arterioles, capillaries, venules (*straight* conduits), and lymphatic capillaries (*curved* conduits). The network configuration changes among organs. Walls of large arterioles and venules contain smooth myocytes that determine flow resistance. The capillary is the smallest blood vessel (caliber range 5–10 μm). It represents a major site for exchange of gases and other substances between the blood and the surrounding interstitial fluid and cells. The capillary wall consists of an endothelial layer surrounded by a basement membrane. A continuous capillary has a complete endothelial lining with tight junctions between endotheliocytes. A fenestrated capillary has fenestrations (pores). A discontinuous or sinusoid capillary has extensive intercellular gaps and incomplete basement membrane. A metarteriole that links arterioles to a venule has distant smooth myocytes that form precapillary sphincters. Postcapillary venules join multiple capillaries from a capillary bed. Arterioles and venules can be surrounded by pericytes

Another homeostatic process is the balance between acidity and basicity (or alkalinity), as enzymes have an optimal pH range, that is, the regulation of arterial blood pH maintained in the narrow range from 7.35 to 7.45 (average or set point 7.4). The maintenance of pH homeostasis, or hydrogen ion control, involves buffering agents that reversibly bind hydrogen ions. Chemical buffers within cells and body's fluids react immediately to control the hydrogen ion (H^+) and hydroxide ion (OH^-) concentrations. Extra- and intracellular buffers include bicarbonate (associated with carbonic acid [H_2CO_3] and sodium bicarbonate [$NaHCO_3$] in the body's fluid), proteins (within cells and blood), and phosphate (NaH_2PO_4 and Na_2HPO_4 in the cytoplasm and urine). Two perfused organs, the lung and kidney, regulate the concentration of these buffers. These organs are responsible for short- ($\mathcal{O}$ [1 mn]) and long-term ($\mathcal{O}$ [1 h]) compensation by modifying the breathing mode and excretion rate of acids (H^+ donors) or bases (H^+ acceptors). For example, carbon dioxide is extracted by lungs during expiration, and bicarbonate ion is excreted by kidneys with urine.

Microcirculation deals with vessel bores of about five to a few hundred μm. Microcirculation, with its four main duct components: arterioles, capillaries, venules, and terminal lymphatic vessels (Fig. 1).

Arterioles correspond to the resistive segment of the vascular tree, where most of the drop in mean pressure occurs. This peripheral resistance is controlled by smooth myocytes, which can widen or narrow the vascular lumen by relaxation or contraction, respectively.

Small precapillary resistance arterioles are richly four innervated by sympathetic adrenergic fibers and highly responsive to sympathetic vasoconstriction via both α1 and α2 postjunctional receptors. It is thus a major site for the regulation of systemic vascular resistance. The primary function is flow regulation, thereby determining nutrient delivery and catabolite washout. They regulate

capillary entry hydrostatic pressure and fluid exchanges.

In some organs, precapillary sphincters can regulate the number of perfused capillaries. Venules are collecting vessels. Sympathetic innervation of larger venules can alter venular tone which controls capillary exit hydrostatic pressure.

Large lymphatic vessels have muscular walls. Spontaneous and stretch-activated vasomotion in terminal lymphatic vessels helps to convey lymph. Lymph circulation is mainly under local control. Smooth myocytes of the stretched lymph vessels, indeed, rhythmically contract at low frequency due to lymph accumulation. Sympathetic nerves cause contraction. Valves direct lymph into the systemic circulation via the thoracic duct and subclavian veins. Lymph flow is very slow. Lymph has a composition similar to plasma but with a small protein concentration. The protein concentration in the lymph is about half that of plasma. Lymphatics have important roles in tissue clearance of molecules, removal of cells from tissues after inflammation, and interstitial fluid homeostasis.

Wall Structure

Small blood vessels of the microcirculation comprise perfusing arterioles, capillaries (caliber 5–10 μm), and draining venules (caliber 8–100 μm).

Arterioles

Arterioles are composed of an endothelium surrounded by one or a few concentric layers of smooth myocytes that regulate blood flow. Arterioles thus have a thin wall. Arterioles receive both sympathetic and parasympathetic innervation.

Capillaries

Capillaries are small exchange vessels composed of endothelium surrounded by a basement membrane.

A capillary bed can encompass two types of vessels: (1) true capillaries which branch mainly from metarterioles and yield mass exchange between cells and blood and (2) a short vascular shunt that directly connects the arteriole and venule at opposite ends of the capillary bed.

Three structural capillary types exist. *Continuous capillaries* in the central nervous system, lung, muscles, and skin are defined by a continuous basement membrane and tight intercellular clefts and have the lowest permeability. *Fenestrated capillaries* in exocrine glands, renal glomeruli, and intestinal mucosa are characterized by perforations in endothelium and thus by relatively high permeability. *Discontinuous capillaries* in the liver, spleen, and bone marrow are defined by large intercellular and basement membrane gaps and, consequently, very high permeability.

Terminal short segment of arterioles with a precapillary sphincter controls the blood entry into that capillary bed. Precapillary sphincters are rings of smooth myocytes at the origin of true capillaries. Mass flux across capillaries depends mainly on six variables: (1) capillary and interstitial hydrostatic pressure, (2) capillary and interstitial oncotic pressure, and (3) filtration and reflection coefficients.

Venules

Many venules unite to form a vein. Venules are composed of an endothelium surrounded by a basement membrane for the postcapillary venules and smooth muscle for the larger venules. Larger venules possess a middle layer of muscular and elastic tissue and an outer tunica of fibrous connective tissue. Venules have thinner walls than arterioles.

High endothelial venules (HEV) are specialized postcapillary venules characterized by simple cuboidal cells. They enable circulating lymphocytes to enter a lymph node.

Pericytes

Pericytes surround the capillaries. They can also encircle precapillary arterioles and postcapillary venules. These periendothelial cells are rich in stress actin bundles.

Differences in pericyte morphology and distribution among vascular bed types can be related to tissue-specific functions (heterogeneous functionality). The pericyte coating (wrapping degree and pericyte density) depends on the perfused organ. The greater the pericyte density, the stronger the microvascular barrier.

Among the types of pericytes, precapillary arteriolar, capillary, and postcapillary venular have different features. Pre- and postcapillary pericytes have actinin (SMC–pericyte transitional cells), whereas capillary pericytes do not.

Pericytes contain smooth muscle (like SMCs) and non-smooth muscle (like endothelial cells) isoforms of actin and myosin. The former has higher levels in pre- and postcapillary pericytes, whereas the concentration of the latter is greater in capillary pericytes.

A basement membrane separates the endothelial cells and pericytes. However, tight and gap junctions can develop between endothelial cells and pericytes. A basement membrane can also be found along the outer surface of the pericytes.

Pericytes, by their contractile function, can regulate capillary bore and then the tissue perfusion, as well as transport from the blood via pericytic processes at interendothelial clefts. Furthermore, pericytes mainly secrete vasoactive autoregulating substances and release structural constituents of the basement membrane and interstitial matrix.

Pericytes produce (1) matrix structural proteins (collagen, fibronectin, laminin); (2) agents involved in clotting and vasculogenesis, such as tenascin, thrombospondin, and plasminogen activator inhibitor; (3) cell adhesion molecules; (4) vasomotor factors such as endothelin-1; and (5) prostaglandins (TXa2, PGi2, PGe2, PGf2α).

Pericytes have plasmalemmal receptors for growth factors (e.g., epidermal growth factor receptor [EGFR] and platelet-derived growth factor receptor PDGFR-β) and various other ligands (e.g., endothelin-1 and histamine receptors) (Shepro and Morel 1993).

Adenosine receptor A2R stimulates adenylate cyclase activity. Adrenergic and muscarinic receptors have also been observed. Signaling leads to the activation of cAMP, transient increase in IP_3, and Ca^{2+} influx. In opposition to smooth myocytes, the membrane potential of the pericyte does not significantly vary after stimulation by ET1, vasopressin, and acetylcholine.

Pericyte coverage is required during angiogenesis. Contacts between endothelial cells and pericytes may control vascular growth, via platelet-derived growth factor and transforming growth factor-β, and endothelium functioning. In cocultures, pericytes modulate endothelial cell proliferation, and the converse is also true.

Pericytes are recruited by endothelial cells that express PDGFb to stabilize the vessel. Pericytes protect the endothelial cell, as they reduce their apoptosis rate.

Cerebral blood flow is strongly regulated to provide 20 % of body energy consumption, even though the brain accounts for only 5 % of total weight, and to match the changing metabolic needs of specific brain regions. Cells that control the blood flow include endothelial and smooth muscle cells, pericytes, neurons, and astrocytes. Contraction and relaxation of the vascular smooth myocytes decreases and increases the artery bore, respectively. Increase in intracellular calcium concentration in astrocytes regulates the arteriole caliber. In the absence of surrounding smooth myocytes, blood flow through capillaries is, indeed, regulated by pericytes that contain contractile machinery (Peppiatt et al. 2006).

About 65 % of noradrenergic innervation of brain blood vessels ends near capillaries rather than near arterioles. Pericyte constriction is associated with a rise in intracellular calcium concentration. Groups of pericytes along capillaries and at capillary junctions of the central nervous system can constrict and relax according to local neuronal activity. Pericyte constriction can hence redirect the blood flow at the capillary level.

Nervous Inputs

Activated 1-adrenergic receptors interact with G q that signals via phospholipase-C leading to (1) diacylglycerol that activates protein kinase-C and (2) inositol trisphosphate that primes calcium influx mainly from the endoplasmic reticulum

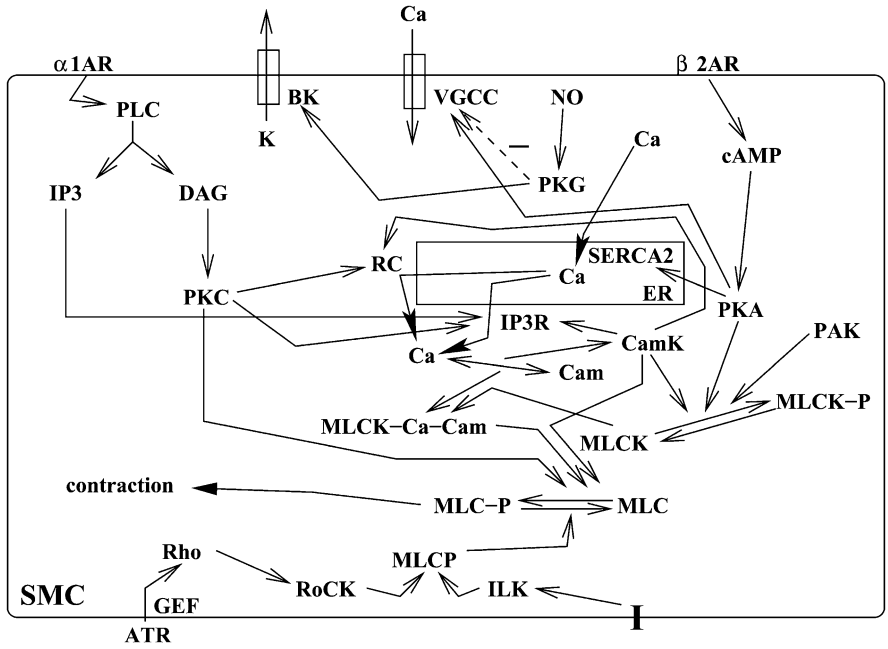

Fig. 2 Contraction of the vascular smooth myocyte and its regulation (Source: Zaugg and Schaub (2004); BK, large-conductance Ca^{2+}-activated K^+ channel; Cam, calmodulin; DAG, diacylglycerol; GEF, GDP-to-GTP-exchange factor; IP_3(R), inositol trisphosphate (receptor); I, integrin; PKA, PKC, protein kinase-A, protein kinase-C; PLC, phospholipase-C; VGCC, L-type voltage-gated Ca^{2+} channel [$Ca_V1.2$]). Adrenergic receptor-1 (α1AR) and adrenergic receptor-β2 (β2AR) cause contraction via the PLC–PKC pathway and relaxation via the cAMP–PKA cascade, respectively. The myosin light chain kinase (MLCK) can be phosphorylated by PKA, PKC, CamK2, and PAK kinases. Myosin light chain phosphatase (MLCP) can be phosphorylated by RoCK and ILK kinases. Phosphorylation of MLCK, which requires Ca^{2+}–Cam, leads to activation, whereas MLCP phosphorylation leads to inactivation. Calcium ATPase SERCA2 is targeted by PKA, and ryanodine-sensitive channel (RC) and its regulatory proteins FKBP and IP_3R are activated by PKA, PKC, or CamK2 kinase. Nitric oxide-induced PKG inhibits $Ca_V1.2$ channel and activates BK channel

(Fig. 2). In vascular smooth myocytes, G-protein-coupled receptor kinase GRK2 that phosphorylates and desensitizes ligand-bound G-protein-coupled receptors impedes vasoconstriction caused by α1d-adrenoceptors (Cohn et al. 2008). β2-adrenergic receptors induce relaxation of vascular smooth myocytes (Table 1).

Smooth muscle myosin-2 consists of two heavy chains and two types of light chains. One part of the heavy chains folds into the globular head that forms the motor domain, and the other constitutes the myosin tail that connects to others to produce the myosin filament. Contraction initiation and termination are switched by myosin phosphorylation by smooth muscle myosin light chain kinase and dephosphorylation by myosin light chain phosphatase. The myosin light chain can also be phosphorylated by PKC and CamK2 kinases.

Table 1 Contraction and relaxation features in the cardiomyocyte and smooth myocyte. The cardiomyocyte is characterized by fast, reversible calcium binding to cardiac troponin-C. Smooth myocyte activity is regulated by reversible phosphorylation of myosin and/or actin components. Vasomotor tone depends on the activity ratio between MLCK and MLCP. β-adrenergic receptor signaling increases intracellular calcium concentration in the cardiomyocyte, whereas its activity in vascular smooth myocyte is independent of calcium

	CMC	SMC
Contraction/relaxation	Fast	Slow
ATP consumption	High	Low
β-Adrenergic signaling	I+	Relaxation

Phosphorylation magnitude determines shortening velocity and tension development. Isoforms

of MLCK in smooth and non-myocytes differ from MLCK in striated myocytes. Myosin light chain kinase can be phosphorylated by PKA, PKC, CamK2, and PAK kinases.

Myosin light chain phosphatase is also phosphorylated (inhibited) by RoCK2 kinase, ensuring a sustained vasoconstriction. Integrin-linked protein Ser/Thr kinase phosphorylates myosin light chain phosphatase as well as myosin light chain.

Regulator caldesmon complexes with actin, tropomyosin, and a Ca^{2+}-binding protein. In the absence of calcium, caldesmon restricts the interaction of the myosin heads with actin. Calcium binding to Ca^{2+}-binding protein relieves the inhibition. Calponin that binds to actin and calmodulin may enhance PKC–ERK1/2 signaling.

Smooth muscle-specific $Ca_V1.2b$ channel is phosphorylated by PKA, PKC, and CamK. Most of the Ca_V channels are packed with Na^+-Ca^{2+} exchanger NCX1, Na^+–K^+ pump, plasmalemmal Ca^{2+} ATPase, and large-conductance Ca^{2+}-activated K^+ channel ($BK_{V,Ca}$).

β-adrenoceptor stimulation activates PKA that, in cooperation with AKAP, phosphorylates Ca_V channels. The cAMP–PKA axis can be counteracted by nitric oxide and its effector protein kinase-G. The latter inhibits Ca_V channels and activates $BK_{V,Ca}$ and MLCP proteins.

Blood–Brain Barrier

Vascular endothelial cells in the central nervous system (CNS) form a barrier that restricts molecule fluxes between the blood and brain. This blood–brain barrier (BBB) ensures proper neuronal functioning and protects the central nervous system. The blood–brain barrier results from interactions between endothelial cells and neural cells. Its main constituents include endothelial cells, astrocytes, and pericytes, in addition to the extracellular matrix.

The average distance from capillary to neuron ranges from 8 to 20 m. The microvasculature of the central nervous system is aimed, in addition to its usual goals, at maintaining the homeostasis of the internal medium, a constant microenvironment being required for neuronal activity.

The blood–brain barrier corresponds to a specialized endothelium of cerebral capillaries that avoids any fluctuation in substance concentration in the extracellular space, especially ions, whereas blood supplies the brain with the required nutrients. Unlike peripheral capillaries that allow substance filtration across and between endothelial cells, the blood–brain barrier strictly limits transport into the brain through cerebral microvascular endothelial cells sealed by tight junctions and having a given distribution of plasmalemmal carriers at its luminal and laterobasal surface. The intercellular cleft width equals about 20 nm. Adjacent cell surfaces fuse. Endotheliocytes of the blood–brain barrier are characterized by transport restriction due to tight junctions and polarized carriers, as well as unique metabolic properties.

Walls of cerebral capillary are thinner than that of the muscle capillary (Coomber and Stewart 1985). The wall thickness could modulate the restrictive permeability of the blood–brain barrier with a shorter transendothelial transport time. A greater mitochondrion number may exist in BBB endotheliocytes than in other endothelial cells, in relation to energy-dependent transcapillary transport (Oldendorf et al. 1977).

The restrictive blood–brain barrier with its enzymes and transporters develops during embryogenesis. Endothelial cells characterized by a reduced vesicular transport form nascent vessels in the central nervous system to which pericytes are recruited, before astrocytes are generated (Daneman et al. 2010). Pericytes regulate the function and proper structure of the blood–brain barrier, in particular the formation of tight junctions and vesicle transfer in endothelial cells of the central nervous system (Daneman et al. 2010). They inhibit the expression of molecules that increase vascular permeability and immunocyte infiltration. Pericytes reduces the permeability of the blood–brain barrier to water and low- and high-molecular-mass molecules (Armulik et al. 2010). In addition, pericytes may mediate the attachment of astrocyte end-feet to endothelial cells (Armulik et al. 2010). The PDGFb–PDGFR complex is required in pericyte recruitment during angiogenesis.

Particle Flow

A particle flow appears in arterioles, the caliber of which equals few tens of m, with a near-wall lubrification zone (plasma layer, thickness $h \sim$ 4–5 μm) and a cell-seeded core. Blood then fills the major part of the microvessel lumen. The cell distribution with a vessel-axis concentration is associated with cell deformation in microvessels.

In capillaries, lumen size ($\leq$10 μm) is smaller than the deformed flowing cell dimension. Blood is nonuniform with a single cell file transported in an axial train of deformed cells (RBC elongation and flexion) with between-cell trapped plasma boli. Blood flow can then be considered as a particle flow slipping on a plasma layer in contact with the endothelium and its glycocalyx.

The arteriolar flow is characterized by the Fahraeus (local hematocrit Ht $<$ global Ht) and Fahraeus–Lindqvist effect (blood viscosity dependence on the hydraulic microvessel radius: $\mu_b(R_h)$) (Fahraeus and Lindqvist 1931). These effects can be explained by a selection between the two phases of blood, plasma, and the blood cell phase, that is, by the interaction of the concentrated suspension of deformable red blood capsules (RBC) with the vascular wall. Red blood capsules localize to the flow core region, whereas a cell-free layer exists near the wall.

In the microcirculation, the local hematocrit decreases with the vessel bore, plasma flowing more quickly than the blood cell phase. The cellular fraction then decreases with respect to that of plasma. The hematocrit within microvessels is then reduced. Hematocrit decreases due to a higher plasma fraction for a given blood volume.

The capillary hematocrit increases when the glycocalyx is removed (Desjardins and Duling 1990). Resistance opposed to the flowing blood in the capillaries can then be due to the glycocalyx (Pries et al. 1997). The glycocalyx is compressed by the moving erythrocytes; fluid can be expelled from this porous material (Feng and Weinbaum 2000).

This phase separation also lowers the viscous dissipation with respect to a suspension of a higher cell concentration in small vessels. In arterioles and venules, the effective blood viscosity then depends on local vessel hydraulic diameter and hematocrit. Interactions between flowing erythrocytes and the capillary wall augment the flow resistance. Blood effective viscosity thus increases in capillaries with respect to that in arterioles and venules.

The plasma peripheral layer also explains the plasma skimming, in particular in the kidneys, where blood filtration occurs. In branching sites, RBC distribution is not uniform. Red blood capsules flow in the vessel with a larger core region.

Blood flow distribution is regulated by arteriole vasomotor tone and pre- and postcapillary sphincter activity. Peripheral blood flow regulation also uses blood vessel recruitment and possible shunts.

Arteriolar Flow

Arteriolar flow is characterized not only by important pressure loss but also by a decrease in inertia forces and an increase in viscous effects. Both the Reynolds number Re and the Stokes number Sto become much smaller than 1. In the microcirculation, the flow velocity v: $\mathcal{O}(10^{-2})$-$\mathcal{O}(10^{-3}$ m/s). As the vessel radius R: $\mathcal{O}(10^{-5}$ m, Re $\ll$ 1, and Sto $\ll$ 1.

Centrifugal forces do not significantly affect the flow in the microcirculation, where the motion is quasi-independent on the vessel geometry.

Venules belong to the intermediary scale of microcirculation. They are merging vessels of similar or different sizes. Junction flow depends on relative vessel size.

Capillary Flow

The capillary circulation is characterized by (1) a low flow velocity (quasi-steady Stokes flow) and (2) a short distance between the capillary lumen and cells.

The capillary wall is adapted to molecular exchanges (Table 2). It is constituted by (1) the

Table 2 Main features of the capillary circulation

Length	0.2–0.4 mm
Radius	4 μm
Between-capillary distance	10–30 μm
Capillary density	300–5,700 (heart)
Total surface	60–1,100 mm^2/mm^3 of tissue (heart)
Volume	10^6 μm^3 (~500 RBCs in a capillary)
Compartmental blood volume	~300 ml (~5 % of total blood volume)
Transit time	0.6–3 s
Pressure	3.5–4 kPa (arteriolar side)
	1.5–2.9 kPa (venular side)
Capillary set flow	100 ml/s
Mean velocity	≤1 mm/s
Hematocrit	<Ht in large vessels (Fahraeus effect)
Viscosity	$\mu = \mu(R_h, Ht)$ (Fahraeus–Lindqvist effect)
Diphasic flow of deformed cells	
Plasma skimming and cell screening	
Flow regulation by recruitment (precapillary sphincter) and possible shunt	

glycocalyx, (2) the endothelium, and (3) a basement membrane.

Endothelium has a variable structure and function according to the type of organ. It is characterized by either pores or intercellular cleft sealed by tight junctions according to the perfused territories.

Large pores represent the vesicular transport through endotheliocytes, sites of apoptotic endotheliocytes, and loci of lost glycocalyx associated with discontinuous tight junctions, in addition to fenestrations without glycocalyx.

The capillary flow locally depends on upstream resistance in arterioles and downstream resistance in venules. Local control of substance transport to the tissue is done by (1) recruitment of terminal arterioles (the higher the number of open capillaries is, the greater the solute delivery and waste removal), (2) possible autoregulation (maintenance of a constant flow despite changing vascular pressure) associated with the cellular activity, and (3) vascular permeability.

Capillary Recruitment

Blood vessel recruitment can refer to angiogenesis that ensures normal tissue growth. Most often, blood vessel recruitment corresponds to the contribution of previously unperfused capillaries to increase the total surface area of mass exchange between the perfused tissue and blood.

Pulmonary Capillary Recruitment

The elevated surface area at the interface between the pulmonary capillary blood and alveolar air by capillary recruitment enables the maintenance of an adequate oxygenation when the metabolic demand rises. Hypoxia augments the cumulative length of perfused capillaries in the pulmonary capillary bed due to the recruitment of previously unperfused capillaries (Wagner and Latham 1975).

In the pulmonary circulation, recruitment has an exclusive capillary origin, as pulmonary arterioles and venules do not participate in the vascular recruitment (Hanson et al. 1989).

The pulmonary capillary recruitment is modulated by pressures in alveoli and up- and downstream vessels, walls of which contain smooth muscle and are innervated, as well as intrinsic factors. The distribution of blood flow within the lung is indeed related to the relation between alveolar, arterial, and venous pressures.

The precapillary pressure influences capillary recruitment. When the postcapillary pressure increases temporarily, the volume of alveolar vessels that constitute an important volume storage heightens (Dawson et al. 1986) and pulmonary vascular resistance decays, as both the small and large vein resistances are reduced (Barman and Taylor 1990).

Intrinsic factors of capillary recruitment rely on activity of local mural cells. Endotheliocytes produce enzymes, such as angiotensin-converting enzyme, 5′-nucleotidase, carboxypeptidase-N, and aminopeptidase-P, that regulate the action of circulating hormones. In particular, circulating angiotensin-1 and bradykinin are processed by enzymes on the luminal surface of pulmonary endothelial cells (Ryan et al. 1975). Angiotensin-1 is converted into vasoconstrictory angiotensin-2,

whereas vasodilatory bradykinin is inactivated. Endothelial cells also synthesize nitric oxide, among other vasoactive substances, to modulate the vasomotor tone, hence the vessel lumen caliber and blood flow resistance.

Transcapillary Transfer of Materials

The capillary endothelium forms a stable antiinflammatory, antithrombotic, and antiadhesive interface between circulating blood components and cells and the body's tissues.

Three fluid compartments exist in series: blood, interstitial fluid, and lymph. According to pressure inside these compartments, water flows continuously from blood to lymph, as walls (i.e., mainly continuous endothelia) of capillaries and postcapillary venules operate as semipermeable membranes. Lymph drains back into the blood circulation via the major veins at the base of the neck.

Water flow across the capillary wall depends on the balance between the osmotic absorption pressure of plasma proteins, or colloid osmotic pressure, and the capillary pressure generated by the cardiac pump.

Microvascular Permeability

The permeability of the microvasculature is a property of its endothelium to govern exchange between blood and perfused tissue. The motion of water and solutes (nutrients and wastes) is driven by a pressure difference balance (difference between the hydrostatic pressure in the capillary lumen and in the interstitium and difference between colloid osmotic pressure in plasma and interstitium [subglycocalyx layer]) for the water convection that conveys molecules as well as concentration gradient for solute diffusion.

The permeability coefficients relate the net fluxes of fluid (water; J_w) and solute (J_s) driven by concentration (c) and pressure (p) differences. Four coefficients are involved: hydraulic conductivity ($\mathcal{G}_h$), diffusional permeability ($\mathcal{P}$), solvent drag coefficient (κ_d), and osmotic reflection coefficient (κ_o) (Michel and Curry 1999).

Mass Transfer Factors

Mass transfer in a microvascular unit between the flowing blood and any irrigated tissue is regulated by (Curry and Adamson 2010) (1) mechanisms that control the number and type of perfusing microvessels, (2) balance between adhesion and contraction in endotheliocytes that determine the conductance of intercellular spaces to water and small solutes, (3) pressure and chemical potential gradients that govern mass transfer, and (4) organization of barriers to macromolecules in the endothelial glycocalyx.

Capillaries are the primary site of exchange for fluid, electrolytes, gases, and macromolecules by filtration and absorption that result from endocytosis as well as diffusion due to the concentration difference and convection due to the pressure difference between the vascular lumen and tissue.

Obviously, fenestrated capillaries have a higher permeability than continuous capillaries. In most capillaries, there is a net filtration of fluid by the capillary endothelium (filtration exceeds reabsorption). Excess fluid within the interstitium is removed by the lymphatic system.

Hydrostatic and Osmotic Pressure

The transport of water and solutes (electrolytes and small molecules) between blood and tissue fluid is mainly determined by two opposing forces, hydrostatic and osmotic transendothelial pressures, as well as endothelium permeability (Fig. 3).

Water flux results from the imbalance between hydrostatic and osmotic pressures for given features of the vessel wall and exchange surface area. A net motion of water out of (positive water flux) or into (negative water flux) the vessel lumen leads to filtration and absorption, respectively. The net driving pressure for fluid motion is determined by the sum of the hydrostatic and osmotic contributions.

The capillary hydrostatic pressure is normally much greater than tissular hydrostatic pressure. The net resulting hydrostatic pressure gradient is positive from the lumen to the tissue in the upstream capillary segment. It drives fluid out of the capillary into the interstitium.

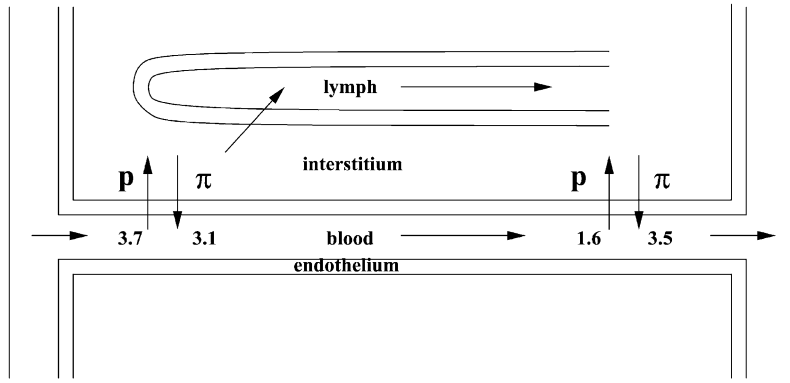

Fig. 3 Capillary exchanges associated with hydrostatic and osmotic pressure value (kPa) distribution

The plasma osmotic pressure is usually much greater than the interstitial osmotic pressure. The resulting osmotic pressure gradient favors fluid reabsorption from the interstitium into the capillary. The osmotic pressure difference must be multiplied by a reflection coefficient associated with capillary permeability to proteins responsible for the osmotic pressure.

In the traditional theory, plasma is filtered out of the capillary entry segment (arterial side) and reabsorbed back into the capillary exit segment (venular side). The ultrafiltrate has the same ion concentration as plasma and does not contain large molecules.

Steady-state equilibrium between the filtration of the arterial side of the microvasculature and reabsorption in venular microvessels (the latter being previously assumed to balance the former) usually does not occur. The balance between the hydrostatic and oncotic pressures is modulated by the control of the interstitial pressure by fibrocytes in particular. Underhydrated glycosaminoglycans can take up fluid and swell, thereby reducing the interstitial pressure (Curry and Noll 2010).

Water Hydraulic Conductivity

The hydraulic conductivity determines the fluid flow per unit pressure gradient across the barrier. In continuous capillaries, water is transported by convection through intercellular clefts of the microvascular endothelium (paracellular route) and, in a smaller but significant proportion (up to 20 %), across the plasma membrane via aquaporins and through the cell (endo- and transcytosis; intracellular route). In fenestrated capillaries (e.g., renal glomerulus), the fenestra is the predominant path that is characterized by a high hydraulic conductivity and larger cross-sectional area than that of the intercellular clefts.

A mixture of low and high molecular weight molecules exerts an osmotic pressure across a semipermeable membrane that is proportional to the size of the channels through which molecules travel. The driving pressure is thus the weighted difference between the hydrostatic pressure difference and colloid osmotic pressure difference between the capillary lumen and the interstitium or subglycocalyx layer.

Solute Permeability

The solute permeability determines the solute flux by diffusion per unit concentration gradient and per unit surface area. In fact, a given solute is transported by both diffusion and convection by water flow driven by a pressure difference between the microvascular lumen and interstitium.

When a porous medium flow theory is used to model the transcapillary exchange and lymphatic removal or the transport of water and solute into biological tissues, the transfer of molecules from the microvascular endoluminal blood actually depends on (1) the interstitial void fraction that varies with the local hydrostatic (interstitial) pressure and the tissue compliance, (2) molecule void fraction, (3) solute diffusivity, (4) tissue hydraulic conductivity, and (5) solvent drag coefficient.

Osmotic Reflection Coefficient

The degree of permeability to a given solute can be quantified by the normalized (ranging 0 to 1 from entirely permeable to wholly impermeable) Staverman osmotic reflection (selectivity) coefficient (κ_o). In other words, the osmotic reflection coefficient of a porous membrane is a measure of the selectivity of the membrane to the solute of interest. "Ideal" solutes have an osmotic reflection coefficient equal to that of the solvent drag.

The sieving coefficient (s) is the inverse of the osmotic reflection coefficient. The sieving coefficient determines the ratio of molecules that is sieved across the membrane. The reflection coefficient (κ_r) is defined as the complementary of the sieving coefficient with respect to unity ($s = 1 - \kappa_r$) (Perktold et al. 2009). Two reflection and sieving coefficients are then considered, the osmotic or solvent drag sieving coefficient ($\kappa_d = 1 - s_d$) and the frictional sieving coefficient ($\kappa_f = 1 - s_f$).

The higher the osmotic reflection coefficient is, the stronger the colloid osmotic pressure in the entrance compartment. An endothelium permeable to water and impermeable to plasma proteins is thus associated with a plasma that exerts a great osmotic pressure that antagonizes the hydrostatic pressure; in the interstitium, both the hydrostatic and osmotic pressures are smaller.

Solvent Drag Coefficient

The capillary blood–tissue interstitium exchange (i.e., the movement of water and proteins through the interstitium by convection and diffusion) depends on the solvent drag effect on solutes. Mass transfer theory is associated with several assumptions: (1) dependence of water flow into tissue on the hydrostatic and osmotic pressure gradient between microvascular blood and tissue, (2) extracellular space changes with variations in local interstitial pressure, and (3) water convection-driven motion of proteins through the tissue at a velocity proportional to the water velocity. Macromolecular (protein) permeability in large pore theory relies on the solute retardation factor, or solvent drag coefficient, in addition to the osmotic reflection coefficient.

If λ_p denotes the ratio between the molecule radius and pore radius and $\phi = (1 - \lambda_p)^2$, the reduction of pore cross section available to the solute and the osmotic reflection and solvent drag coefficients in the pores are computed using the following equations (Perktold et al. 2009):

$$\kappa_{o,p} = (1 - \phi)^2, \tag{1}$$

and

$$\kappa_{o,p} = \frac{16}{3}\lambda_p^2 - \frac{20}{3}\lambda_p^3 + \frac{7}{3}\lambda_p^4. \tag{2}$$

Endothelial Barrier

The endothelium and its associated structures, e.g., the glycocalyx, basement membrane, junctions between apposed endotheliocytes, and supporting pericytes, form the primary barrier to water and plasma protein motion, thereby maintaining the plasma volume and venous return. Nevertheless, it enables transvascular exchange to fulfill the local metabolic needs.

Adherens and Tight Junctions

The tight junction is a nearly continuous band that consists of transmembrane proteins: junctional adhesion molecule (JAMa), claudin, and occludin. In the cytosol, tight junction proteins are connected to actin filaments via zona occludens ZO1 and ZO2 proteins.

These junctional strands, especially in the inner segment (near the wetted surface) of the intercellular cleft, limit outward water flow and create a difference between colloid osmotic pressures in the subglycocalyx space and interstitial fluid.

In fact, the endothelial tight junction strand is not continuous, but contains infrequent breaks (length 100–400 nm). These breaks occur at 2–4 m intervals, thereby forming large pores and, hence, unrestricting passage of molecules through intercellular spaces. Therefore, water as well as solutes such as plasma proteins is funneled through these breaks.

Adherens junctions strengthen intercellular adhesion by a homophilic Ca^{2+}-dependent

transinteraction of cadherin-5 (or vascular endothelial [VE] cadherin) as well as junctional adhesion molecules (JAMa–JAMc). In the cytosol, adherens junction proteins are anchored to cortical actin filaments that reside around the perimeter of each cell via catenins (Ctnnα–Ctnnδ).

Therefore, cell adhesion molecules, such as cadherin-5 and occludin, stabilize the endothelial barrier. On the other hand, both adherens and tight junctions are tethered to the cortical actin cytoskeleton via several adaptors, such as catenins and zona occludens proteins, respectively.

Furthermore, vascular endotheliocytes are also anchored to the extracellular matrix via focal adhesions supported by integrins and actin-linking proteins, such as paxillin, talin, and vinculin.

Endotheliocyte Adhesion and Contraction

The endothelial barrier relies on a balance between intercellular and cell–matrix adhesions that maintain the integrity of the barrier and stress fiber contraction within endotheliocytes that opens intercellular gaps.

Myosin light chain kinase (MLCK) phosphorylates myosin light chain, principally MLC2, in response to Ca^{2+} binding to MLCK-associated calmodulin, thereby supporting actomyosin contractility, weakening interendothelial cell adhesion, and causing vascular hyperpermeability via gap formation (Shen et al. 2010).

Once it is activated by Ca^{2+}-calmodulin or phosphorylation by protein Tyr kinase (Tyr464 and Tyr471), MLCK phosphorylates MLC (Ser19 and subsequently Thr18) (Shen et al. 2010).

On the other hand, myosin light chain phosphatase (MLCP) dephosphorylates MLC, hence relaxing the cytoskeleton. Activated RhoA GTPase stimulates RoCK kinase that subsequently phosphorylates (inhibits) MLCP, thereby increasing endothelial permeability.

Endothelial hyperpermeability mediated by MLCK in response to histamine, thrombin, and VEGF relies on PKC activation as well as NO production and subsequent priming of the sGC–cGM–PKG–cRaf–ERK1/2 pathway (Shen et al. 2010).

Cortical Actin Cytoskeleton

Cellular junctional complexes are stabilized by inhibition of cofilin and recruitment of ubiquitous cortactin. Unphosphorylated cofilin binds to ^{F}actin and promotes filament severing, thereby destabilizing the cortical actin cytoskeleton. Kinase LIMK phosphorylates (inactivates) cofilin.

On the other hand, cortactin is implicated in cortical actin assembly, reorganization, and strengthening. Cofilin phosphorylation regulates cortical actin fibers.

Glycocalyx

The glycocalyx layer at the interface between blood and the vessel wall constitutes the first barrier that is permeable to water and solutes, but retains plasma proteins and inflammatory leukocytes in the vascular space, before any trans- or paracellular transfer.

The glycocalyx excludes circulating blood cells and macromolecules. Hindrance of fluid and solute radial transfer, or conversely permeation of proteins into the glycocalyx, depends on the molecule size and charge as well as on the glycocalyx fiber size, orientation, and spacing, limiting accessibility to small plasma molecules. The glycocalyx is able to restrict access of blood-borne agents by both size and electrostatic exclusion. It reduces albumin permeability from a magnitude order of 10^{-6} cm/s in the absence of the glycocalyx to that of 10^{-7} cm/s (albumin reflection coefficient close to 0.9) (Curry and Adamson 2010).

The Fahraeus effect (i.e., a microvascular hematocrit lower than the macrovascular hematocrit) associated with a central flow where red blood capsules accumulate and a peripheral plasma layer (width 0.4–0.6 μm) in contact with the glycocalyx that moves with a slower velocity than the mean RBC velocity can be explained not only by phase separation of RBCs and plasma at upstream bifurcations but also exclusion of circulating RBCs and plasma by the glycocalyx.

The glycocalyx can be considered as a negatively charged gel-like mesh of glycosaminoglycans (glypican, hyaluronan, and syndecan-1) and sialoglycoproteins. These molecules extend from

40 to 600 nm from the endothelial luminal membrane. The scaffold of the glycocalyx is formed by anionic polysaccharides (glycosaminoglycans, proteoglycans, and glycoproteins).

Heparan sulfate proteoglycans contain abundant binding sites for plasma proteins. Their core proteins, syndecans and glypicans, can function as signal transducers. The glycosaminoglycan hyaluronan, which is not sulfated and lacks binding sites for proteins, contributes significantly to the volume of the glycocalyx due to its hydration capacity.

The endothelial glycocalyx contains a relatively thin layer of membrane-bound macromolecules and a relatively thick layer of adsorbed plasma components. Plasma proteins, endothelial-derived growth factors, enzymes, and water are adsorbed within the polysaccharidic mesh.

The glycocalyx coats the inner wetted surface of capillaries, including the entrance of the intercellular cleft and most fenestrations. It operates as both a determinant of vascular permeability and mechanotransducer. A sustained physiological shear participates in the maintenance of a stable endothelial phenotype.

Intercellular Cleft

Endothelial cells overlap along their perimeter by a distance of 0.1 to more than 1 μm. Therefore, the lateral edge is not perpendicular to the wetted surface, but oblique.

The cleft between apposed endotheliocytes follows a long, narrow, tortuous path. The cleft is sealed by porous tight junctions. The width of the interendothelial cleft (18–22 nm) is determined by transmembrane adhesion proteins such as cadherin-5 that provides a homophilic link between adjoining cells.

The paracellular passage is the primary route for water and solute exchange across the microvascular wall when gaps form between apposed cells. In the cardiac microvasculature, venules possess tight junction strand breaks as well as much smaller gaps (Curry and Adamson 2010). The permeability of these venules reaches the upper values reported in mammalian microvessels.

Transcytosis

The capillary endothelium contains plasmalemmal vesicles (size 60–80 nm). Caveolae invaginate from the luminal plasma membrane and form vesicles carried along the cytoskeleton that fuse with the abluminal plasma membrane. Caveolae are coated by the integral membrane protein caveolin-1 on their cytoplasmic face.

Other vesicular transport means can also contribute to transendothelial transfer of materials.

Interstitium

Blood capillaries are surrounded by a loose connective tissue that contains a given interstitial fluid volume. The extracellular matrix consists of 4 main components: (1) a fibrous collagen network that serves as a scaffold, (2) fibrous elastin meshwork, and (3) ground substance formed from proteoglycans composed of glycosaminoglycans linked to proteins as well as the free glycosaminoglycan hyaluronan.

Interstitium acts as a storage space for the fluid filtered across the capillary wall. The interstitial fluid is an ultrafiltrate of plasma with a total protein concentration of 50–60 % of plasma level and with an electrolyte composition similar to that of plasma.

The composition of the interstitial fluid depends on the transcapillary fluid flow, itself function of the quality of the capillary wall barrier, and molecule size and charge.

Several matrix components (e.g., chondroitin and heparan sulfate and hyaluronan) are cleared out from the interstitium by an elevated fluid flow. The turnover rate that depends on clearance and synthesis rate varies according to the organ type.

Interstitium is a dynamical structure that can participate in transcapillary water filtration via a modulation of the interstitial fluid pressure. The latter is the filling pressure for initial segments of lymphatics.

Vasodilation

Increased nutrient exchange relies on the regulation of both perfusion and permeability. In fact, it depends more on vasodilation that raises the

exchange surface area and associated augmented water-driving pressure (endoluminal and hence transparietal pressure) and elevated concentration differences between blood and tissue than a marked increase in permeability (Curry and Noll 2010).

Vasodilation increases the number of microvessels perfused during exposure to an inflammatory agent as well as the permeability on blood–tissue exchange of fluid and solutes. Nitric oxide elevates permeability of the microvascular bed. On the other hand, vasoconstriction attenuates these effects.

The heparan sulfate-rich glycocalyx layer limits perfusion volume in capillaries and hinders transparietal fluid and solute transport. Vasoactive substances can alter glycocalyx exclusion ability (VanTeeffelen et al. 2010). Vasodilators such as adenosine and bradykinin operate at the level of the glycocalyx rather than by increasing the local blood flow. Adenosine provokes shedding of hyaluronan from the glycocalyx (VanTeeffelen et al. 2010).

Monomeric GTPases in the Maintenance of the Endothelial Barrier

Cell adhesion stabilizers target small (monomeric) GTPases. These effectors contribute to the organization of the cortical actin cytoskeleton and distribution of constituents of endothelial adherens junctions. Small GTPases are activated by guanine nucleotide-exchange factors (GEF) and inactivated by GTPase-activating proteins (GAP).

The maintenance of the microvascular barrier depends on various types of small GTPases, in particular Rac1, CDC42, and RhoA proteins. Both Rac1 and CDC42 are the main monomeric GTPases that protect the endothelial barrier (Spindler et al. 2010). They are antagonized by RhoA regulator.

Effect on Cytoskeleton Dynamics

Both Rac1 and CDC42 GTPases activate via PAK1 and PAK4 LIMK enzyme (Spindler et al. 2010). On the other hand, the RhoA effector RoCK kinase inhibits LIMK, hence favoring cofilin-mediated ^{F}actin depolymerization.

In addition, RhoA GTPase destabilizes the endothelial barrier via RoCK kinase that inactivates myosin light chain phosphatase (MLCP) as well as phosphorylates MLC, hence increasing MLC phosphorylation and provoking actin–myosin fiber contraction.

However, both Rac1 and RhoA GTPases can also have opposite effects. For example, the microvascular endothelial barrier is destabilized by Rac1 during angiogenesis. In addition, Rac1 acts via PAK to enhance MLC phosphorylation in macrovascular endothelial cells. On the other hand, RhoA can strengthen endothelial cortical actin via its effector Dia in a profilin-dependent manner.

Microtubule Participation

Microtubule polymerization stimulates RhoA, thereby increasing permeability of endothelial cell monolayers. Once it is uncoupled from microtubules, the microtubule-associated protein RhoGEF2 targets RhoA, a mechanism used by thrombin (Spindler et al. 2010).

Effect on Cell Junctions

IQ motif-containing GTPase-activating protein IQGAP1 impedes α-catenin–β-catenin binding, hence preventing ^{F}actin linkage to adherens junctions (Spindler et al. 2010). Both Rac1 and CDC42 may regulate cadherin-mediated cell adhesion by sequestering IQGAP1 inhibitor.

A loss of cell adhesion can result from phosphorylation mainly by SRC family kinases and endocytosis of cadherin–catenin complex components (Spindler et al. 2010). Several barrier-destabilizing mediators, such as VEGF, thrombin, and TN-FSF1, signal via small GTPases such as Rac1 and provoke phosphorylation of cadherin-5 and β- and δ1-catenin. Activator RhoGEF2 connects to the tight junction complex via the adaptor cingulin; it augments endothelial permeability.

cAMP Mediator

Monomeric Rac1 GTPase activated by sphingosine-1-phosphate enhances peripheral localization of cadherin-5 as well as α- to γ-catenins as well as reduces stress fiber formation, but promotes cortical actin assembly (Curry and Adamson 2010).

Sphingosine-1-phosphate elevates the cytosolic concentration of cAMP messenger.

Prostaglandin-E_2 and prostaglandin-I_2 as well as atrial natriuretic peptide (ANP) elevate cytosolic cAMP concentration, hence promoting Rac1 and CDC42 activation via the RapGEF3-Rap1 pathway and TIAM1 and Vav2 GEFs (Spindler et al. 2010).

The barrier protector cAMP operates via Rap1-mediated activation of Rac1 and CDC42 as well as RhoA inhibition. Messenger cAMP acts via RapGEF3 and RapGEF4 that stimulate Rap1 and indirectly activate Rac1 GTPase. The cAMP–RapGEF–Rap1 axis stabilizes the peripheral actin band.

Mediator cAMP activates not only Rac1 but also synergistically CDC42 via Vav2 protein (Spindler et al. 2010). Stabilization of the endothelial barrier by oxidized phospholipids relies also on CDC42 GTPase. In addition, CDC42 is a major GTPase involved in barrier restoration.

Molecule cAMP represses effect of TGF-β that disorganizes the microtubular mesh and, hence, increases endothelial permeability likely via RapGEF3 activator.

Nitric Oxide

The path through small pores of tight junctions can be modulated, in particular by nitric oxide (Curry and Adamson 2010). Once it is synthesized by nitric oxide synthase-3 and released in response to inflammatory agents, such as bradykinin, platelet-activating factor (PAF), and vascular endothelial growth factor (VEGF), nitric oxide increases microvascular permeability (Durán et al. 2010).

The signaling pathway involved in hyperpermeability comprises soluble guanylate cyclase (sGC), cGMP, and protein kinases PKC and PKG as well as ERK1 and ERK2.

Platelet-activating factor that activates NOS3 increases endothelial permeability, but does not cause vasodilation. On the other hand, some vasodilators such as acetylcholine (ACh) activate NOS3, but do not alter the microvascular permeability (Durán et al. 2010). Both PAF and ACh separate NOS3 from caveolin-1, but ACh promotes preferential movement of NOS3 to the Golgi body, whereas PAF favors its motion in the cytosol.

In endotheliocytes, NOS3 localizes mainly to the plasma membrane and Golgi body, but also distributes in the cytosol. Its localization to plasmalemmal caveolae relies on ^{N}myristoylation and palmitoylation. It translocates from the plasma membrane to subcellular compartments upon demyristoylation and depalmitoylation, thereby relieving the inhibitory connection with caveolin-1 (Durán et al. 2010). It is internalized with caveolae.

However, both membrane-bound and cytosolic NOS3 are able to release nitric oxide, the former form releasing more basal NO than cytosolic form (Durán et al. 2010). Its relocalization to specific subcellular compartments determines its function as well as access to arginine pools and scavengers of reactive nitrogen species, thereby ensuring protection, as NO is also a radical.

Its activity is determined by multiple mechanisms: (1) activating and inactivating phosphorylation and dephosphorylation of specific NOS residues (Ser116, Ser617, Ser635, Ser1179, Thr497, and Tyr83), (2) ^{S}nitrosylation that prevents NOS3 activity and reduces sensitivity of sGC to NO activator, (3) interaction with different proteins, and (4) specific subcellular localization.

Activation of NOS3 in response to proinflammatory stimuli responsible for microvascular hyperpermeability proceeds from (1) translocation from the plasma membrane to cytosol via caveolae and (2) dissociation from caveolin-1, association with heat shock protein HSP90, Ca^{2+}–calmodulin binding, phosphorylation (Ser1177), and dephosphorylation (Thr495) (Durán et al. 2010).

Insulin-like and vascular endothelial growth factor as well as hemodynamic stress can increase permeability of venules via protein kinase-B that phosphorylates (activates) NOS3 (Ser1177). Bradykinin stimulates calmodulin-dependent kinase CamK2 that also phosphorylates NOS3 (Ser1177).

VEGF

Vascular endothelial growth factor (VEGF), previously called vascular permeability factor and

vasculotropin, regulates vascular permeability. In humans, the VEGF family includes five gene products (VEGFa to VEGFd and placental growth factor [PlGF]). Isoform VEGFa, or VEGF, is synthesized in almost all cells subjected to hypoxia or other stress types. These proteins signal upon binding to their cognate receptors, in particular VEGFR1 to VEGFR3, once they homo- and heterodimerize. They operate as a potent (but not very powerful) endothelial growth factor, a powerful vascular permeabilizing agent, and a potent vasodilator.

It signals via VEGFR2, calcium influx through Ca^{2+} store-independent transient receptor potential (TRP) channels TRPC3 and TRPC6, as well as Ca^{2+} store-dependent TRPC1, phospholipase-Cγ, Src kinase, protein kinase-Cα, the cRaf–MAP2K1/2–ERK1/2 module, nitric oxide synthase, guanylate cyclase, the Rho–Rac axis, cadherin, zona occludens, and occludin (Bates 2010).

It can act as a stimulator or inhibitor of endothelial cell proliferation. It promotes transfer by vesiculo-vacuolar organelles and reduces the cell adhesion molecule content at endothelial junctions, which causes a loss of tight and adherens junctions, thereby enhancing mass transfer by both trans- and paracellular routes. In addition, it supports the formation of fenestrations (Bates 2010).

Subtype VEGFa binds to VEGFR1 and VEGFR2. It favors albumin extravasation. Proangiogenic splice variants of VEGFa (e.g., $VEGFa_{165A}$) increase also the hydraulic conductivity (Bates 2010). Antiangiogenic VEGFa isoforms such as $VEGFa_{165B}$ can also raise the hydraulic conductivity via VEGFR1 receptor.

Subtype VEGFc binds to VEGFR2 and VEGFR3. It augments the hydraulic conductivity acutely via VEGFR2 receptor.

The other VEGF family member, placental growth factor (PlGF), binds only to VEGFR1 receptor. It does not increase the hydraulic conductivity acutely (Bates 2010).

Mass Transfer

Very thin-walled capillaries represent the major exchange zone, where blood velocity is low. In this exchange region, the quantity of interest is the transit time of conveyed molecules and cells. The mean residence time in a circulatory compartment is the ratio of substance–cell holdup to the flow rate in the compartment.

Solute can be transported by either diffusion or convection through gaps of fenestrated capillaries. A fraction of filtrated plasma is sucked back from the interstitial liquid into capillaries, and the remaining part is drained by lymphatic circulation into large veins.

Materials that cross the vessel wall include respiratory gases, water, ions, amino acids, carbohydrates, proteins, lipid particles, and cells. The capillary permeability is high for water and moderate for ions, lipids, and proteins.

Fluid can move from the intravascular compartment to the extravascular space composed of cellular, interstitial, and lymphatic subcompartments. Water motion into or out of the capillary, across the endothelium, is partially driven by osmosis. Water moves from regions of low solute concentration to regions of higher solute concentration. The metabolic activity of endotheliocytes contributes to water motion.

The osmotic pressure is the pressure required to stop the net flow of water across a membrane separating solutions of different composition. The Van't Hoff equation describes the osmotic pressure on one side of the membrane. It is valid for a single chemical species of concentration c: $\Pi = R_g T c$, where R_g is the perfect gas constant and T the temperature. A given solution can lead to different osmotic pressures when the filtration membrane porosity differs. The osmotic pressure (Π) depends on wall features.

In a capillary in which the intraluminal pressure drop Δp_i is linear and the tissue pressure (p_{tis}) constant and the capillary wall are semipermeable, the solvent transport due to $\Delta p = p_i - p_{tis}$ is diminished by $\Delta\Pi$ due to the presence of macromolecules in the capillary lumen that do not cross the wall. When the local effective pressure associated with osmotic and hydrostatic pressure differences between the lumen and the wall (subscript lw) $p_{eff} = \Delta p_{lw} - \Delta\Pi_{lw} > 0$, the plasma is filtrated. When $p_{eff} < 0$, the plasma is reabsorbed from the interstitial fluid. In normal conditions,

the filtration rate equals the sum of the reabsorption rate and lymphatic flow rate.

Transcapillary fluid exchange through fenestrated capillaries and across the glycocalyx and within the intercellular cleft in continuous capillaries can rapidly adjust.

As the tissular fluid volume is three to four times larger than the plasma volume, the tissular fluid serves as a reservoir that can supply additional fluid to the circulatory apparatus or draw off excess.

Inflammation and Edema

Inflammatory and allergic reactions are characterized by an altered endothelial barrier. During inflammation, microvascular permeability is selectively increased in small postcapillary venules.

During inflammation, the glycocalyx and intercellular junctions are acutely modified. Inflammatory mediators increase vascular permeability primarily by the formation of intercellular gaps in venules, once adherens and tight junctions open. Inflammatory gaps (size <1 μm) form at intercellular sites in venules (Curry and Adamson 2010).

Alteration of Glycocalyx

The near-wall flow region in the microvasculature can be decomposed into (1) the glycocalyx, a carbohydrate-rich, blood-excluding intraluminal layer that contributes to a low capillary hematocrit, and (2) a cell-free plasma layer. The core region carries blood cells.

Exclusion by the endothelial glycocalyx of flowing cells and molecules is reduced by adenosine and other vasoactive substances (VanTeeffelen et al. 2010).

Vesicular Transfer

Increased endothelial permeability caused by platelet-activating factor (PAF) is counteracted by NOS inhibition and reduced NO production. This mechanism explains inhibition of caveolin-1 that directly interacts with NOS3 enzyme. Caveolin-1 action on microvascular permeability is antagonized by an elevated endothelial cytosolic Ca^{2+} concentration (Zhou and He 2010). Caveolin-1 and endothelial Ca^{2+} level antagonistically regulate Ca^{2+}–calmodulin-dependent NOS3 activity.

Degradation of Adhesion Sites

Microvascular permeability is modified by altering adhesion sites between apposed endotheliocytes as well as between them and the extracellular matrix.

Histamine, thrombin, and VEGF disturb the endothelial barrier (Rabiet et al. 1996). Thrombin disrupts the Cdh5-Ctnn complex in adherens junctions. Cadherin-5 and occludin undergo marked widespread rearrangement with a local loss of adhesion proteins at intercellular junctions.

The bacterial endotoxin lipopolysaccharide disrupts endothelial tight junctions. Cytokine TNFSF1 breaks the endothelial barrier at cell adhesion supported by cadherin-5 (Spindler et al. 2010).

Intercellular Gap Formation

In cultured endothelial monolayers most often stimulated by thrombin as an acute inflammatory stimulus, paracellular gap formation is blocked upon inhibition of RoCK or MLCK, but not in situ. Thrombin launches an active cell RhoA-dependent contraction that creates large gap formation and, hence, an acute increase in endothelial barrier permeability. Some of the effects of thrombin on vascular permeability result from the release of other inflammatory mediators from mastocytes or neurons. Thrombin primes a contraction-dependent increase in permeability (Curry and Adamson 2010). In addition, thrombin activates platelets that contribute to elevated endothelial permeability.

Whereas RoCK kinase, myosin light chain kinase (MLCK), and myosin ATPase are implicated in cell contraction during formation of endothelial gaps in cell cultures, occurrence of gaps in vivo in mesenteric venules in response to bradykinin does not depend on this mechanism (Curry and Adamson 2010). Likewise, platelet-activating factor raises endothelial permeability in a cell contraction-independent manner in inflamed rat mesentery venules.

The transmembrane glycoproteic adamalysin subtype ADAM15 is involved in vascular inflammation. Its production is upregulated upon exposure to proinflammatory cytokines. This inflammatory mediator increases endothelial permeability in response to thrombin via the Src–ERK1/2 pathway that supports endothelial cytoskeleton contraction and, hence, intercellular gap formation (Sun et al. 2010). This effect is independent of FAK activation as well as disruption of adherens junctions and focal adhesions (i.e., connections between integrins and matrix constituents) and shedding of ectodomain of cell adhesion molecules (e.g., cadherin-5 and integrin). Enzyme ADAM15 promotes also neutrophil transendothelial migration (Sun et al. 2010). Neutrophils migrate across the endothelium via the paracellular route maintained by junctional molecules (e.g., cadherin-5, PECAM1, and JAMa).

Reduction of cAMP Concentration

Inflammatory mediators raise endothelial permeability. They disrupt the endothelial barrier, at least partly, as they reduce near-membrane cAMP concentration. Messenger cAMP actually enhances the barrier function, because it activates Rac and Rap1 GTPases to stabilize the barrier, independently of PKA kinase (Curry and Noll 2010). On the other hand, RhoA GTPase promotes cytoskeleton contractility, thereby augmenting endothelial permeability.

The cAMP concentration is regulated by phosphodiesterases, especially PDE2a and PDE3a. The other messenger cGMP inhibits PDE3a, but activates PDE2a, hence its bimodal regulation (Curry and Adamson 2010). At low concentrations (<100 nmol), cGMP inhibits PDE3a without activating PDE2a, thereby raising cAMP level and lowering endothelial permeability. At higher concentrations, cGMP activates PDE2a, overcoming effects of PDE3a inhibition, thereby diminishing local cAMP level and increasing endothelial permeability.

Similarly, at a low concentration, atrial natriuretic peptide triggers synthesis of cGMP at a low intracellular level and attenuates endothelial permeability, whereas a higher ANP concentration increases endothelial permeability (Curry and Adamson 2010).

Activation of Phospholipases

Upon receptor binding, proinflammatory agents activate phospholipases PLA2, PLC, and PLD, as well as Ca^{2+} channels (Durán et al. 2010).

Activated PLA2 via the lipoxygenase axis leads to the formation of leukotrienes, particularly LTc_4, that activate NOS enzyme. Via the cyclooxygenase axis, PLA2 activates thromboxane synthase (hence, vasoconstriction caused by platelet-activating factor).

Phospholipase-C catalyzes the synthesis of inositol trisphosphate and diacylglycerol, hence releasing Ca^{2+} from intracellular stores and activating protein kinase-C. The latter phosphorylates (inactivates) NOS3 (Thr495). In addition, PKC may phosphorylate (activate) cytoskeletal proteins, such as caldesmon and vimentin, as well as myosin light chain kinase. Moreover, an imbalance in activity of PKCβ2 and PKCδ contributes to the endothelial hyperpermeability (Durán et al. 2010).

Reactive Oxygen Species

In addition, products of activated leukocytes such as reactive oxygen species increase the permeability. Platelet adhesion to sites where the endothelial barrier is opened initiates the inflammatory cascade, the strong interaction of platelets with leukocytes enhancing activation of leukocytes. In fact, endotheliocytes, leukocytes, platelets, macrophages, and mastocytes interfere via their products (cytokines, chemokines, and ROS) (Curry and Noll 2010).

Hyperpermeability and Edema

Once the control of the microvascular permeability is lost, the endothelium becomes hyperpermeable. During inflammation, capillaries become even leaky; water volume within interstitium thus increases and leads to tissue swelling or edema.

In addition, the interstitial fluid pressure lowers down to -1.33 kPa (-10 mmHg; the normal capillary filtration pressure ranging from 65 to 133 Pa [0.5–1 mmHg]), thereby increasing the capillary filtration (Reed and Rubin 2010).

Inflammatory agents regulate the microvascular permeability using endothelial-dependent and endothelial-independent mechanisms, as they act also on fibroblasts and lymphatics of the microvascular unit (Curry and Adamson 2010).

Excessive accumulation of water in interstitium is due to a lack of reabsorption into capillaries and/or in filtration into lymphatics. In fact, the edematous interstitium can result from (1) an increased capillary and venous hydrostatic pressure associated with heart failure or venous obstruction, (2) decreased plasma osmotic pressure, (3) increased capillary permeability caused by proinflammatory mediators and damaged leaky capillaries, and (4) lymphatic obstruction.

Microvascular Permeability and Leukocyte Adhesion

Protein leakage from plasma to tissue is temporally and spatially dissociated from leukocyte adhesion and endothelial transmigration during inflammation (He 2010). Leukocyte adhesion and migration are thus uncoupled from microvascular permeability changes. After exposure to inflammatory stimuli, most of the adherent or migrating leukocytes that take the paracellular route (i.e., not through activated endothelial cells) are observed at intercellular junctions of postcapillary venules distinct from endothelial gaps. Both solute leakage and leukocyte adhesion occur in the early phase, but leakage lasts longer than the transient leukocyte adhesion. Although both platelet-activating factor and leukotriene-B_4 cause leukocyte adhesion, only the former augments the fluid filtration, as LTb_4 exposure does not alter endothelial barrier (He 2010). In addition, leukocyte transmigration involves only a transient opening of adherens junctions. Altered cadherin-5 during cell migration quickly diffuses back to reseal the gap.

On the other hand, production primed by cytokines and release of reactive oxygen species from stimulated neutrophils increases the microvascular permeability.

In addition, during inflammation, platelets support leukocyte recruitment and elevated microvascular permeability. Platelet interaction with venular endothelial cells is initiated by endothelial gap formation (He 2010). In inflamed venules, platelet–endothelium interaction mediated by P-selectin recruits additional leukocytes. Consequently, ROS production is amplified and enables a sustained increase in microvascular permeability.

Microvascular Permeability

Exchange vessels aim at supplying dissolved gases, ions, and solutes to cells, after transferring these low molecular weight molecules across the vessel wall.

Except liver, adrenal, and bone marrow sinusoids, in which the endothelium has large pores, the vascular endothelium constitutes a selective barrier between blood and tissue. A filter at the luminal entrance to endothelial clefts provides low permeability to macromolecules. In most microvessels, the macromolecular transport is done by transcytosis (vesicular mass transfer) and not through porous clefts. Microvascular exchange is mainly passive.

Endothelial cells have tight junctions that limit the vascular permeability. The strength of these intercellular connections is controlled by various messengers to modulate the vascular permeability, in addition to vascular growth and repair. The stability of the tight junction depends in particular on RhoA guanosine triphosphatase, itself activated by Rho guanine nucleotide-exchange factors.

Angiopoietin-1 and vascular endothelial growth factor VEGFa strengthen and disrupt tight junctions, respectively. They determine the localization of the RhoA-specific guanine nucleotide-exchange factor PlekHg5 to control RhoA activity at tight junctions, hence endothelial permeability (Ngok et al. 2012). Angiopoietin-1 supports PlekHg5 recruitment to tight junctions, thereby stabilizing cell adhesion. Protein PlekHg5 is recruited to cell junctions by adaptor and scaffold members of the Crumbs polarity complex at sites of intercellular contacts (adherens and tight junctions as well as synapses) and promotes junction integrity by activating diaphanous. Diaphanous inhibits cadherin-5 endocytosis and Src activity.

On the other hand, VEGFa activates protein kinase-D1 that phosphorylates (Ser806; inactivates) PlekHg5, thereby reducing PlekHg5 tethering to its junctional anchors and removing it from cell junctions (Ngok et al. 2012).

Exchanges of Water and Hydrophilic Solutes

The hydraulic conductivity measures the porosity of the capillary wall for the water flux. The filtration coefficient is the hydraulic conductance per unit exchange surface area.

Nutrients and metabolic wastes are transported between blood and cells by convection associated with fluid motions and diffusion according to the pressure and concentration gradients, respectively. Molecular transfer is facilitated by the very slow blood flow in the capillary (i.e., by a high residence time).

Diffusion from a compartment of higher concentration to a region of lower concentration across a membrane of infinitesimal thickness is governed by the Fick law. Brownian motion states that the substance flux is proportional to the solute permeability coefficient, which depends on the diffusivity and solubility of the investigated solute, transport surface area, and concentration gradient.

The selectivity coefficient, or reflection coefficient, measures the probability of solute penetration across the vessel wall. A selectivity coefficient equal to 1 means that the vessel wall is impermeable to the molecule. Most plasma proteins does not penetrate (reflected off) the barrier; they are responsible for the osmotic pressure. A selectivity coefficient equal to 0 means that transport is not restricted. Small solutes, such as salts and glucose (selectivity coefficient 0.01), are easily transferred. In the range bounded by these two values, the wall layer is semipermeable to solute with some amount that hardly penetrates the barrier (strong reflection).

In microvessels with a continuous endothelium, the main route for water and solutes is the endothelium cleft, except when tight junctions exist. Transcapillary water flows and microvasculature transfer of solutes, from electrolytes to proteins, in both continuous and fenestrated endothelium, can be described in terms of 3 porous in-parallel routes: (1) a water pathway across endothelial cells, (2) a set of small pores (caliber 4–5 nm), and (3) a pool of larger pores (bore 20–30 nm) (Michel and Curry 1999).

The estimated exchange area between apposed cells is on the order of 0.4 % of the total capillary surface area. The array of junctional strands between endothelial cells is interrupted at intervals, allowing water and solute fluxes. Loss of the glycocalyx in regions of discontinuous tight junctions between adjacent cells can form localized nonselective regions (large pores) without widening of intercellular junctions.

The pore theory simulates the cleft passages between adjacent endothelial cells in continuous endothelium. The pore density is defined by the effective fraction of the cleft width used for molecular exchange. The pore size is determined by the interfiber spacing in a fiber matrix at the cleft entrance.

The associated fiber matrix model of capillary permeability associated with the endothelium glycocalyx (thickness $\sim$100 nm; fiber spacing 7 nm) provides a basis for molecular size selectivity, especially in a fenestrated endothelium. A thin matrix at the cleft entrance can indeed be a major determinant of the permeability properties of the capillary wall. Such a fiber matrix model can also be applied to the cleft itself because large portions of the cleft contain matrix components. Models have predicted that the fiber layer (typical thickness 100 nm), which extends from the endothelium surface into the cleft entrance region, sieves solutes (Weinbaum and Curry 1995).

The entire membrane permeability coefficient is the sum of the different route coefficients. The membrane selectivity coefficient is the sum of the individual coefficients of the in-parallel paths weighted by the fractional contribution of each path to membrane hydraulic conductivity. Despite its limitations, the pore theory is a useful pedagogical tool. Moreover, any fiber matrix-based modeling must take into account not only fiber size and volume but also matrix organization (Michel and Curry 1999).

The effective pore radius, a selectivity measure, is determined by interstices in the fiber

matrix, which depend on matrix composition and arrangement. The effective pore number is determined by the size and frequency of endothelium passages in the intercellular spaces as well as through cells.

Water and small solutes can indeed cross endotheliocytes, using specific channels. Aquaporins (Aqp) are membrane water-transport proteins (Agre et al. 1995). Subtype Aqp1 is found in endothelia. However, the contribution of the transcellular transfer to the net flux is supposed to be small. In most microvessels, aquaporins contribute to less than 10 % of the hydraulic conductance, except in the blood–brain barrier and possibly skeletal muscle capillaries (Michel and Curry 1999). Aquaporins intervene when interstitial osmolarity increases such as in renal descending vasa recta.

An elevated transmural pressure on endothelial cell culture on a porous rigid matrix increases the endothelial hydraulic conductivity (Tarbell et al. 1999). Augmented shear stress in endothelial cleft resulting from heightened transmural flow raises the hydraulic conductivity via a NO–cAMP-dependent mechanism.

Macromolecule Permeability

Macromolecules can cross the endothelium between cells (paracellular transport) or preferentially through endothelial cells (transcytosis), using proper receptors, specific or not, and vesicles.

Vacuole-like structures can be observed, isolated inside the endotheliocyte, as luminal membrane invaginations, or connected to the abluminal compartment (Chen et al. 1998). Both luminal and abluminal surfaces of the capillary endothelium are dynamical with invaginations and protrusions associated with environmental stimuli. Moreover, vesicle translocation between luminal and abluminal membranes is accelerated when the transendothelial pressure rises. The endothelial permeability can increase by vesiculo-vacuolar organelles without formation of trans- or intercellular gaps.

The macromolecule flux from blood to interstitium can mainly occur in postcapillary venules because their endothelial cells have simple intercellular junctions.

Microvascular wall models comprise pores for small- and intermediate-sized molecules and transendothelial channels for macromolecules. The macromolecular transport, which is independent of convection, needs endothelial vesicles, a mass transfer mechanism that uses cytoskeletal tracks and their coupled nanomotors, and a more efficient process than diffusion.

Transport Laws

The fluid volume flux per unit endothelial area J (or J_w; subscript w: water), also called volumetric flow rate per unit area and volume filtration rate per unit area, across the endothelial barrier that is modeled by a membrane is given by the Starling relation:

$$J(\kappa_o = 0) = \mathcal{G}_h(\Delta p - \Delta \Pi), \tag{3}$$

where $\mathcal{G}_h$ (dimension: $M^{-1}.L^2.T$) is the hydraulic conductivity or capillary filtration coefficient, $\Delta p = p_\ell - p_{int}$ the difference in hydrostatic pressures between capillary lumen (p_ℓ [3.3-3.7 kPa (25–28 mmHg)]) and interstitial fluid (p_{int} [2.0-2.2 kPa]), $\Delta \Pi = \Pi_\ell - \Pi_{int}$ the difference in osmotic (oncotic) pressures between capillary lumen (Π_ℓ) and interstitial fluid (Π_{int}), and κ_o osmotic selectivity (reflection) coefficient of the vessel wall for the chemical species of interest ($\kappa_o = 0$ if the endothelial membrane is fully permeable to transported molecular species and $\kappa_o = 1$ if the membrane is impermeable).

Therefore, volumetric filtration rate per unit endothelial area increases when (1) the capillary hydrostatic pressure rises, (2) the interstitial hydrostatic pressure lowers, (3) the capillary colloid osmotic pressure decays, and/or (4) the interstitial colloid osmotic pressure augments. The transcapillary water flow contributes to transendothelial solute flux.

Because both the plasma and interstitial fluid contain many solutes (molecular species $_i$), the water movement across the capillary wall can be written as (Levick and Michel 2010)

$$J_w = \mathcal{G}_h\left(\Delta p - \sum \kappa_{o_i} \Delta \Pi_i\right). \tag{4}$$

In most microvascular beds, only concentrations of macromolecular solutes differ between the plasma and interstitial fluid. Hence, J_w can be described approximately by the difference between the effective osmotic pressure exerted by macromolecules in plasma and interstitial fluid.

The Kedem–Katchalsky equations incorporate convection and diffusion:

$$J_w = \mathcal{G}_h(\Delta p - \kappa_o \Delta \Pi), \tag{5}$$

$$J_s = \mathcal{P}\Delta c + J_W(1-\kappa_d)c_*, \tag{6}$$

where subscripts w and s stand for water and solute, respectively, $\mathcal{P}$ (dimension: $L.T^{-1}$) the membrane diffusional permeability for the solute, Δc the difference in solute concentration across the endothelium (between the plasma and interstitial fluid just beneath the endothelium), c_* the averaged solute concentration within the pore that represents the endothelial cleft, and κ_d the dimensionless solute drag reflection coefficient that depends on membrane permeability for both water and solute.

The quantities Δp and $\Delta \Pi$ are driving and hindering forces for water flow (i.e., volume transport that convects a given solute), respectively. The quantity Δc is the driving force for diffusive solute transport. The quantities $\mathcal{G}_h$ (order 10^{-7} cm/s/cm H_2O both in vivo and in vitro conditions), $\mathcal{P}$ (values of which vary between in vivo [order 10^{-8}–10^{-7} cm/s for albumin] and in vitro [order 10^{-6} cm/s for albumin; order 10^{-7} cm/s for 70-kDa dextran] microvascular endothelium (Tarbell 2010)), κ_o, and κ_d are transport properties. The endothelial transport properties are sensitive to both the chemical and mechanical environment.

The relative contribution of convection and diffusion is given by the dimensionless transport parameter ($\mathcal{T}$) (Tarbell 2010)

$$\mathcal{T} = \frac{\mathrm{Pe}}{\exp\{\mathrm{Pe}\} - 1}, \tag{7}$$

where Pe is the Péclet number that is defined by

$$\mathrm{Pe} = (1-\kappa_d)\frac{J_w}{\mathcal{P}}. \tag{8}$$

The Péclet number is the ratio of the velocity at which the macromolecular species is washed by convection (solvent drag) to its diffusive velocity in the endothelial barrier.

Therefore, the solute transport equation can be written as

$$J_s = (\mathcal{P}\mathcal{T} + (1+\kappa_d)J_w)\Delta c. \tag{9}$$

When the solute transport is dominated by convection, $\mathrm{Pe} \gg 1$, $\mathcal{T} \to 0$, and $\mathrm{Pe} \to (1-\kappa_d)J_w$. When the solute transport is dominated by diffusion, $\mathrm{Pe} \ll 1$, $\mathcal{T} \to 1$, and $\mathrm{Pe} \to \mathcal{P}$.

The fluid volume in the interstitial space is assumed to be regulated within a narrow range by readjustment of the interstitial hydrostatic and colloid osmotic pressures according to capillary and lymphatic conditions. However, the interstitial fluid pressure (p_{int}) is an active force that creates a fluid flux across the capillary wall particularly in inflammation.

Limitations of the Starling Law

The traditional form of the Starling principle governing microvascular fluid exchange between plasma and the interstitial fluid across the endothelial barrier related to the balance between hydrostatic and oncotic pressures must be modified due to variations of interstitial pressures and the semipermeable glycocalyx (Reed and Rubin 2010; Levick and Michel 2010).

The classical filtration–reabsorption model that relies on a spatial fluid balance does not describe fluid exchange in the real microcirculation, because (1) both p_{int} and Π_{int} change when J_w varies and (2) the composition of the subglycocalyx fluid diverges from that of the bulk interstitial fluid (Levick and Michel 2010).

The tissue fluid balance in the lung, muscle, and skin, among others, is not achieved by an equilibrium between upstream filtration and downstream reabsorption in the steady state. The drainage of the capillary filtrate by lymphatic vessels is thus the dominant factor of the interstitial volume homeostasis. However, the globally

averaged net filtration constraint is much smaller than the hydrostatic–osmotic pressure balance.

The arteriolar vasomotion cycles may support the lymphatic drainage. Arteriolar contraction lowers the capillary pressure and promotes transient fluid absorption, whereas the arteriolar relaxation favors filtration, thereby creating a temporal fluid balance (Levick and Michel 2010). In addition, the net filtration force across the capillary endothelium depends more on the colloid osmotic pressure below the endothelial glycocalyx than that in the bulk interstitium.

Filtration Rate–Osmotic Pressure Relation

Microvascular absorption is only transient in capillaries with a low blood pressure (i.e., in most tissues); a slight filtration can prevail even in venules (Levick and Michel 2010). Starling relation states that the filtration rate drops when the capillary concentration of plasma proteins rises or when the interstitial concentration of plasma proteins diminishes, for a given difference in transendothelial fluid pressure.

In some specialized organs (e.g., kidney and intestine), fluid absorption is associated with local epithelial egress of plasma proteins from the interstitium to the lymphatic system.

Absorption in capillaries with a low blood pressure is observed only transiently. The concentration of plasma proteins in the interstitial fluid (plasma protein filtrate concentration; c_{int}) is inversely related to the capillary filtration rate, because the interstitial fluid is continually renewed, and the interstitial concentration of plasma proteins is determined by the rate of solute influx (J_s) relatively to the rate of water flow influx (J_w; extravascular dilution curve) (Reed and Rubin 2010; Levick and Michel 2010):

$$c_{\text{int}} = J_s / J_w. \tag{10}$$

When the capillary filtration rate rises, interstitial and lymph macromolecules are diluted, hence their concentration falls. The pericapillary colloid osmotic pressure is thus inversely related to the filtration rate.

The low rate of filtration and lymph formation in most tissues can be explained by the plasma protein concentration gradient within the intercellular cleft of continuous capillaries and around fenestrations, the subglycocalyx space.

Subglycocalyx Space

The interstitial fluid at the glycocalyx abluminal side is separated from the pericapillary interstitium by tortuous intercellular clefts with gaps through tight junctions. A gradient of plasma protein concentration can arise along the cleft. Therefore, the difference of colloid osmotic pressure across the capillary barrier in Starling law is defined by that between the capillary lumen and the subglycocalyx space rather than the difference of colloid osmotic pressure between the capillary lumen and the bulk interstitial fluid:

$$J_w = \mathcal{G}_h \left[(p_\ell - p_{\text{int}}) - \kappa_o \left(\Pi_\ell - \Pi_{\text{sg}} \right) \right], \tag{11}$$

where Π_{sg} is the colloid osmotic pressure in the subglycocalyx space.

The colloid osmotic pressure in the subglycocalyx space of the ultrafiltrate sieved by the glycocalyx can be small because κ_o is high and the outward ultrafiltrate flow through the narrow breaks in the intercellular junctional strands prevents protein diffusion equilibrium between the subglycocalyx and pericapillary fluid (Levick and Michel 2010). Differences between plasma protein concentrations in the subglycocalyx space and pericapillary medium depend on the magnitude of the capillary filtration pressure (p_ℓ). The effective osmotic pressure difference opposing fluid filtration may equal Π_ℓ rather than $\Pi_\ell - \Pi_{\text{int}}$ term of Starling law, when Π_{sg} is very low. Therefore, the basal volumetric filtration rate per unit endothelial area is balanced by the lymph drainage rate (Levick and Michel 2010).

Varying Interstitial Pressure

In addition to adjustability of the gradients of plasma protein levels across the glycocalyx and within the intercellular cleft in continuous capillaries as well as around fenestrations, the extracellular matrix and interstitial fluid pressure influence the transcapillary exchange.

Cells exert a tension on the extracellular matrix constituents. The interstitial fluid pressure (p_{int}) depends on the interstitial volume and bulk modulus:

$$B = \frac{\Delta p_{int}}{\Delta V_{int}/V_{int}}, \quad (12)$$

where V_{int} is the interstitial volume. A decreased interstitial fluid pressure increases the transcapillary fluid flow that, in turn, augments the solute convection across the capillary wall.

In turn, an elevated capillary filtration heightens the interstitial fluid pressure and reduces the interstitial colloid osmotic pressure, thereby limiting further filtration augmentation. This automatic readjustment is called capillary filtration autoregulation by the interstitial pressure (Reed and Rubin 2010).

The interstitial fluid pressure acts as the filling pressure that increases lymph flow in initial lymphatics. In addition, the interstitial exclusion, that is, the fact that plasma proteins do not have access to the full interstitial volume due to steric exclusion by structural matrix molecules, influences the time at which a new steady state is reached (Reed and Rubin 2010). A higher exclusion lowers the interstitial content of plasma proteins, thereby reducing the time at which a new steady state occurs. Moreover, lymph flow increases until a steady state is achieved. The enhanced removal of protein associated with the lymph clearance reduces the protein amount.

Cellular tension on the extracellular matrix in cooperation with matrix fiber networks restrains expansion of the glycosaminoglycan gel, thereby keeping the interstitial fluid pressure at a relatively high value.

Upon removal of the cellular tension exerted on the collagen and microfibrillar networks in the connective tissue via the collagen-binding β_1-integrins, glycosaminoglycans of the ground substance that are normally underhydrated can expand and take up water (Reed and Rubin 2010).

On the other hand, several growth factors and cytokines such as PDGFbb (but neither PDGFaa nor FGF) can cause the contraction of fibroblasts and restore the matrix compaction and a high interstitial fluid pressure via α_V β_3-integrin as well as phosphoinositide 3-kinase and protein kinase-C (Reed and Rubin 2010).

Insulin and prostaglandin-$F_{2\alpha}$ can also renormalize the interstitial fluid pressure. On the other hand, proinflammatory substances, such as IL1 and TNFSF1, as well as prostaglandins PGe1, PGe2, and PGi2 (prostacyclin), attenuate the matrix cell contraction and collagen gel compaction and decrease the interstitial fluid pressure.

In the skin, macrophages of the connective tissue exert a control of the interstitial fluid volume using tonicity-responsive enhancer-binding protein (TonEBP) (Reed and Rubin 2010). The latter binds to the promoter of the VEGFC gene, thereby leading to VEGFc secretion by macrophages and avoiding interstitial hypertonic volume retention during high-salt diet. Factor VEGFc may act as an osmosensitive regulator that contributes to the handling of sodium balance.

Epithelial Mass Transfer in the Kidney, Lymph Node, and Gut

In peritubular capillaries of the renal cortex and ascending vasa recta of the renal medulla, in intestinal mucosal capillaries, and in lymph nodes, fluid is absorbed continuously (Levick and Michel 2010). In the kidney and intestine, the interstitial fluid is renewed by a release of protein-free fluid by the epithelium.

In the rat ileum, the pressure in fenestrated capillaries of the mucosa is much lower than that in continuous capillaries of circular and longitudinal smooth muscles. In cats, the intestinal lymph flow increases, and its protein concentration decreases as fluid is absorbed from the small intestine lumen. During the absorption of digested food, the epithelial absorption of glucose and amino acids is confined to the outer third of the villus; fluid absorbed through epithelium may be taken up into the extensive capillary bed of the inner two-thirds of the villus and lacteals.

In the renal cortex, the low interstitial plasma protein concentration and, hence, interstitial colloid osmotic pressure are maintained by the low macromolecular permeability of the fenestrated peritubular capillaries and the fast production of

a protein-free interstitial fluid by the tubular epithelium, which flushes the relatively small amount of plasma protein entering the cortical interstitial fluid into lymphatics (efficient lymphatic drainage) (Levick and Michel 2010).

In the renal medulla, fluid absorbed by the collecting duct from the nascent urine is cleared continuously from the medullary interstitial fluid to the ascending vasa recta. Fenestrated ascending vasa recta, unlike fenestrated cortical peritubular capillaries, have a relatively high permeability to plasma proteins. Albumin is cleared from the medullary interstitial fluid and directly taken up into medullary capillary blood (countercurrent exchange) by protein convection (Levick and Michel 2010).

In lymph nodes, the interstitial fluid is continuously replaced by the inflowing prenodal lymph of low protein concentration (Levick and Michel 2010). The rapid renewal of the interstitial fluid counteracts the inverse relation between the capillary filtration rate and colloid osmotic pressure.

Transmural Transport Modeling

Three main stages are involved in material transport to and across the vessel wall. Stage 1 deals with transport in the vessel lumen. Once conveyed at the possible site for transendothelial migration, the particle must cross the near-wall fluid domain. Going from intraluminal blood to the vessel wall, the particle crosses the diffusion boundary layer. The thickness of the diffusion boundary $\delta \propto \left(\mathcal{D}_z/\gamma_w^{\cdot}\right)^{1/2}$, where $\mathcal{D}$ is the species effective diffusion coefficient and z the distance downstream from the inlet.

Certain molecules circulate either more or less freely in the plasma or linked to erythrocytes. Both transport modes can be used by the same molecule, such as albumin. The partition coefficient between plasma and RBC inner fluid depends on molecule diffusivity and RBC membrane permeability. Such process is usually not taken into account in literature models.

In addition, the axial dispersion of the tracers in the vessel lumen can be limited by the radial diffusion (Taylor 1953, 1954; Aris 1956). The longitudinal dispersion of a tracer slug with respect to the cross-sectional average concentration is describable as diffusion in the longitudinal direction with diffusivity $\mathcal{D} + R^2 V_q^2 (48\mathcal{D})$.

Stage 2 corresponds to material uptake by the wall luminal surface and transendothelial transport. Molecules must cross the glycocalyx and either the endothelial cell or the cleft. Adsorption is shear-dependent and can require material conversion. Some lipoprotein conformations, which depend on the wall shear stress, are more convenient for irreversible adsorption, which affects the exchange rate at the interface. The final stage 3 focuses on transmural transport.

Transport models are currently focused on inner wall layers, neglecting the adventitia and its blood irrigation and drainage. Data on blood adventitial convection to and from the vessel wall remain unknown. Moreover, the studied part of the wall supposes that the wall is composed of a set of layers separated by membranes.

Transport through any wall layer is based on convection and diffusion. Convection refers to solvent-guided solute motion under a given transtunica pressure. The filtration pressure through the vascular porous wall is the difference between the luminal and external pressure (i.e., atmospheric pressure for superficial blood vessels). The pressure distribution across the vessel wall remains unknown as well as its dependence with luminal pressure. Increase in blood pressure can induce permeability changes due to porous medium compaction. Diffusion is associated with a concentration gradient. The vasomotor tone can also affect the material transfer through the wall poroviscoelastic interstitial matrix. Molecule transport through elastic laminae depends on their fenestrae size, which can vary with applied stresses. In the media, elastic fenestrated lamellae are also perpendicular to the flux axis. Main transport-associated phenomena are (1) hindrance due to friction during solute displacement, (2) solute reflection associated with local partial permeability of the medium to be crossed, and (3) possible reactions.

The solvent (water, subscript w) and solute (subscript s) transports across the vessel wall

Table 3 Mass transport coefficients and relations. An effective porosity is introduced because collisions between solid parts of the porous medium (length scale L^*; volume V, with solvent volume V_w) and solute slow the transport (V_{weff}, available solvent volume for solute). J_s, solute flux per unit surface area

Parameter	Relationship
Darcy filtration speed	$J_w \equiv \breve{v}_D(\Delta\Pi = 0) = -(\mathcal{P}_D/\mu_D)/\nabla_p = G_h\Delta_p$
$\breve{v}_D \cdot 24em\left[\mathrm{L.T^{-1}}\right]$	(Darcy law)
Hydraulic conductivity	$\breve{v}_D(\kappa_o = 0) = G_h\left(\Delta_p - \Delta\Pi\right)$
G_h [$\mathrm{M^{-1}}$.$\mathrm{L^2}$ .T]	(Starling law)
Darcy permeability	
$\mathcal{P}_D[\mathrm{L^2}]$	
Drag reflection coefficient	$\kappa_d(\Delta c = 0) = 1 - J_s\left(J_w\breve{c}\right)$
Osmotic reflection coefficient	$\kappa_o(J_w = 0) = \Delta p/\Delta\Pi$
Porosity	$\Psi = V_w/V$
Effective porosity	$\psi = V_{weff}/V$
Solute permeability $\mathcal{P}$	$J_s(J_w = 0) = \mathcal{P}\Delta\Pi$
Solute diffusivity $\mathcal{D}$	$J_s(v = 0) = \mathcal{D}\Delta c$ (first Fick law)
	$\kappa_h\breve{v}\cdot\nabla\breve{c} - \mathcal{D}_{eff}\nabla^2\breve{c} = 0$ (second Fick law)
Slip transport	
If $\Psi > 0.8$ and $L^* < P_D^{1/2}$	$\nabla_p = -(\mu_D/\mathcal{P}_D)\breve{v}_D + \mu_D\nabla^2\breve{v}_D$ (Brinkman equation)

require transport variables, such as the hydrostatic Δp and osmotic $\Delta\Pi$ pressure difference across the wall layer, as well as physical control parameters such as the hydraulic conductivity (G_h), permeability ($\mathcal{P}$), porosity (Ψ, i.e., the ratio between the fluid volume and the fibrous matrix volume), diffusivity ($\mathcal{D}$), osmotic (κ_o), and solute drag (κ_d) reflection coefficients, related to the solute selectivity of the wall tunica interfaces, hindrance coefficient (κ_h) (Table 3).

Hindrance coefficients are associated with collisions between molecules and solid walls (Prosi et al. 2005):

$$c_t + \nabla\tilde{n}(-\mathcal{D}\nabla c + \kappa_h v c/\psi) = 0. \qquad (13)$$

The wall-layer porosity Ψ is supposed to be time-independent. An example of literature values is given in Table 4.

Literature Data

Wall absorption of substances and transport through the vessel wall have been investigated to study capillary exchanges and inadequate efflux of accumulated substances through fenestrated internal elastic lamina and the media to the adventitial blood and lymph vessels.

Diffusion can be the dominant transmural mass transfer mechanism rather than convection (Caro et al. 1980). Nonetheless, transmural convection, which depends on the wall stress field, influences the macromolecular transport within the arterial wall (Tedgui and Lever 1985).

Another objective was to determine the transfer-limiting step of the entire process. Stage 1 does not provide a dominant resistance to material motions (Caro and Nerem 1973). However, vessel curvature induces local variations in blood-wall mass transfer rate (Kaazempur-Mofrad and Ethier 2001).

The vascular endothelium provides a priori a major transport resistance and hence determines the transmural flux. The other wall layers affect the material distribution. The wall porosity is layer-dependent due to layer composition and structure. The layer influence depends on the molecule type. The media that has a greater transport resistance for albumin than the adventitia acts as a barrier for this molecule (Caro et al. 1980).

Table 4 Values of wall transport coefficients for albumin (diffusivity of 9×10^{-11} m^2/s and inlet concentration of 572 nmol/cm^3) in a 2D model of an artery (caliber of 6 mm and length of 12 cm) (Manseau 2002). The inlet velocity profile is parabolic, and the lumen, intima, and media *Pe* are, respectively, equal to 1.2, 1.7, and 7.1. The wall layers are supposed to be homogeneous. The endothelium and internal elastic lamina are modeled by continuous semipermeable membrane crossed by convective and diffusive fluxes. Permeability coefficients are derived from a pore model (Curry 1984). Transport coefficients in the subendothelial space of the intima and the media are based on a fibrous matrix model (Huang et al. 1994)

	Endothelium intima	IEL	Media
	Porous media		
h (μm)	10		300
$\mathcal{P}_D$ (m^2)	9×10^{-17}		5×10^{-20}
D_{eff} (m^2/s)	6×10^{-11}		2×10^{-12}
κ_h	1.12		3.08
	Membranes		
G_h (m/Pa/s)	3.6×10^{-12}	3×10^{-10}	
P (m/s)	5.5×10^{-10}	6.4×10^{-9}	
κ_o	0.75	2×10^{-3}	
κ_d	0.75	2×10^{-3}	

Wall ingress-controlled or wall egress-controlled mechanisms are disturbed in vascular wall lesions. Four factors are involved in disturbed mass transport that leads to atherosclerosis: blood hypoxemia, leaky endothelial junctions, transient intercellular junction remodeling, and convective clearance of the intima and media (Tarbell 2003). High LDL transport is found to be correlated to low O_2 transfer to promote intimal thickening (Ethier 2002). Proposed models generally do not take into account the different biochemical processes involved in vessel lumen and wall mass transport such as molecule binding, degradation, etc. Neglect of O_2–hemoglobin bonds has been found to lead to large errors in O_2 transfer using a simple one-layer wall model (Moore and Ethier 1997).

Transport Models

Dealing with mass transfer in the artery wall, literature models focus on solute dynamics from the vessel lumen across the wall intima and media, separated by internal elastic lamina. Therefore, the role of external elastic lamina and adventitia with its blood and lymph vessels is usually neglected.

The computational domain is divided into three main compartments: the vascular lumen, intimal subendothelial region, and media. The endothelium and internal elastic lamina define the interfaces between these subdomains. Solute transport between the different subdomains is coupled by mass flux across the interfaces (Table 5).

Transport models aimed at describing solute transport across the different layers of the artery wall must handle suitable quantitative data for the whole set of physical-involved parameters. The advection–diffusion equation (ADE) describes the solute transport in the vessel lumen, the convection term being provided by the local blood velocity field obtained by solving the Navier–Stokes equations:

$$c_t + \mathrm{v} \cdot \nabla c + \nabla \cdot (D \nabla c) = 0, \qquad (14)$$

where c is the studied species concentration. Endothelium is usually assumed to be a semipermeable membrane with pores corresponding to junctions and leaky cells. Normal junctions are represented by circular sections around normal endothelial cells with a pore set in its central region; leaky junctions are modeled by rings around leaky cells (Tsay et al. 1989).

Blood flows are currently assumed to be laminar, either steady fully developed in a straight rigid stented artery (Manseau 2002; Garon et al. 2001; Grant 2004) or unsteady 3D (Rappitsch et al. 1997) but with questionable parameter values (Garon et al. 2001).

Mass transport across the subendothelial layer of the intima and media is modeled by the convection–diffusion–reaction equation. Fluxes J across the endothelium and the internal elastic lamina are computed using Kedem–Katchalsky equations:

$$\begin{cases} J_{\mathrm{w}} = G_h(\Delta p - k_o \Delta \Pi), \\ J_s = P \Delta c + J_{\mathrm{w}}(1 - k_d)\breve{c}_* \end{cases} \qquad (15)$$

Table 5 Transluminal and transmural transport (Source: Fry (1987))

Transport layer	Layer thickness (μm)	Governing equations (main quantity)
Vessel lumen	Variable	Advection–diffusion equation (c)
		Navier–Stokes equation (v)
Endothelium	0.5–2	Kedem–Katchalsky equation (J)
Glycocalyx	0.1–0.25	Usually non-modeled
Subendothelium (intima)	5–10	Darcy equation $\left(\breve{v}_D\right)$
		Advection–diffusion–reaction equation $\breve{c}$
IEL	2–5	Kedem–Katchalsky equation (J)
Media	300–1,000	Darcy equation $\left(\breve{v}_D\right)$
		Advection–diffusion–reaction equation $\breve{c}$
EEL		Usually non-modeled
Adventitia		Uptake by blood and lymph
		Non-modeled

($\breve{c}_* = \Delta c/\ln(c_2/c_1)$: averaged concentration at interface).

The subendothelial space of the intima is assumed to be a homogeneous porous media composed of a fibrous matrix with proteoglycans and collagen fibers. In a porous medium, the pressure and velocity are averaged in representative elementary volume greater than the pore size and smaller than the domain size. The volume-averaged filtration velocity $\breve{v}_D$ across any wall layer is computed using the Darcy law (Re $\ll 1$) and a Darcy permeability coefficient P, a tensor reduced to a scalar in isotropic homogeneous media.

The two intima constituents, proteoglycans and collagen fibers, with their respective volume fraction V_{PoG} and V_{Cn}, are supposed to be in series (Grant 2004):

$$P^{-1} = P^{1}_{\mathrm{PoG}} + P^{1}_{\mathrm{Cn}}. \tag{16}$$

The permeabilities for proteoglycans and collagen fibers are computed using the Carman–Kozeny equation, which needs the values of the fiber radius, porosity of the fiber matrix, and Kozeny constant.

Diffusion transport in porous media obeys to Fick law, the diffusion resulting from a concentration gradient in a moving solvent. The effective diffusivity depends mainly on proteoglycans (Michel and Curry 1999).

The internal elastic lamina is supposed to be a thin semipermeable membrane composed of fenestrae of given radius, given density, and consequently, given relative surface area. Its conductance ($G_{h,\mathrm{IEL}}$) is derived from the geometry variables of the internal elastic lamina and its fenestrae, as well as its permeability (P_{IEL}) (Curry 1984). The mass transfer-associated coefficients κ_o and κ_d are also given in the literature (Curry 1984; Anderson and Malone 1974).

The media is assumed to be a homogeneous porous media composed of a fibrous matrix and smooth myocytes. Effective coefficients can be obtained from the literature (Curry 1984; Wang and Tarbell 1995; Huang and Tarbell 1997).

The convection–diffusion–reaction provides the volume-averaged concentration $\left(\breve{c}\right)$. The concentration decrease in the vessel wall is mainly due to the endothelium (82 % (Manseau 2002), 68 % (Rappitsch et al. 1997)).

A substance transport model in the microvasculature has been developed (Beard and Bassingthwaighte 2000). The model is based on basic hexagonal network units composed of a set of parallel capillaries that are periodically arranged in the plane, with cross connections to sources in arteriolar zones and sinks in venular regions. The arteriolar and venular zones belong also to a periodic structure in the direction normal to the cross section of the capillary set, the centers of mass of adjacent zones being separated by a distance of 500 m. Tracer transport based on the convection–diffusion equation is coupled to the flow distribution.

Simulation of the Chemical Coupling

The arterial wall has a selective permeability for blood solutes. Its transfer depends strongly to the local flow behavior. The Navier–Stokes equations provide the velocity and pressure fields and then the convection term for the solute transport. The Navier–Stokes equations are coupled to the convection–diffusion equation for the solute concentration in the vessel lumen. Not only the solute transport within the vessel lumen depends on the velocity field, but also the boundary conditions of the solute transfer on the endothelium are related to wall velocity gradient. The near-wall solute diffusion is associated with a diffusivity tensor, which depends on wall shear stress. The mathematical and numerical modeling of the coupling problem of the lumen transport and the transfer across the rigid endothelium have been analyzed (Quarteroni et al. 2002a).

ADE is coupled to transport equation to model wall mass transfer. The Beavers–Joseph–Saffman condition can be used at the interface between the vessel flow and the porous medium (Jäger and Mikelić 2000). Inside the arterial wall, a pure diffusive dynamics is commonly considered. The coupling problem has been solved in an axisymmetric stenosis, using the Brinkman model (extension of the Navier–Stokes equations for porous media; Table 6), assuming a wall made of a single homogeneous layer (Stangeby and Ethier 2002). Splitting in the lumen advection–diffusion equation in the wall diffusion equation has been associated with an efficient iterative method based on a Steklov–Poincaré interface equation (Quarteroni et al. 2002b). Numerical techniques for transport in large artery lumen and wall are presented in (Zunino 2004). Multilayered wall models require determination of numerous physical parameters. The parameter set can be obtained from measurement fitting using electric analogues (Prosi et al. 2005). Numerical results depend on values of transport coefficients in membranes and porous media, which are roughly estimated, generally from in vitro experiments and associated modelings.

Convective Heat Transfer

Convective heat transfer by the blood acts in homeothermy of the human body. Circulatory heat exchangers and conservers allow the heat or cooling of the body, depending on environment and body conditions, heat being convected by blood circulation. During exercise, the body temperature rises.

The main exchange surfaces (with a given thermal conductivity) are the lungs and skin. Blood heat is transferred to alveolar air to be exhaled to environmental air across the exchange barrier, the thin alveolocapillary membrane, or the skin with its numerous cell layers.

Heat exchangers can be bypassed, especially in the limbs with two venous networks, the superficial under the skin and the deep accompanying arteries, with anastomoses between them.

Cancer treatments can use thermal ablation, which is less invasive than surgery. Therapy efficiency depends on the local blood flow. Image-guided radiofrequency ablation treats cancers particularly localized to the liver, kidney, and adrenal glands by heating. One or more radiofrequency needles are inserted into the tumor. Cryotherapy uses gas-refrigerated cryoprobes, which are inserted inside the tumor, initiating the formation of ice balls to destroy cancerous cells by freezing and thawing processes. One of the main difficulties is the determination of the optimal position of the probes and

Table 6 Transport in porous media

Scale	Model	Equation
Macroscopic	Darcy	$-\nabla p = (\mu/P)\,\breve{v}$
Mesoscopic	Brinkman	$-\nabla p = (\mu/P)\,\breve{v} - \mu\nabla^2\,\breve{v}$
Microscopic	Navier–Stokes	$-\nabla p = \rho Dv/Dt - \mu\nabla^2 v$

treatment duration for complete destruction of cancerous cells without damaging too many surrounding normal cells. Another kind of tumor therapy consists of thermal and mechanical exposure to high-frequency focused ultrasound (HIFU). Tumor antigens and other compounds released from destroyed cells can stimulate antitumoral immunity. The optimal exposure time is an important parameter to avoid damage of normal cells, especially walls of neighboring blood vessels.

Heat transfer models use heat source(s) and sink(s) and effective conductivity to describe the thermal influence of blood flow. A continuum model cannot account for the local thermal impact of the vasculature, with countercurrent vessel segment pairs. The vasculature must also be modeled, down to a certain caliber, and be combined with a continuum model for heat transfer in the irrigated tissues.

The bioheat transfer equation proposed by Pennes in 1948 is used in physiological heat transfer modeling dealing with the microcirculation (Pennes 1948). The Pennes model provides the rate of heat change in a given body tissue from the sum of the net heat conduction into the tissue, metabolic heat generation, and heating (or cooling) effects of the arterial supply. Pennes underestimated the magnitudes of the conduction and convection terms in the energy balance, using inappropriate values of tissue thermal conductivity and tissue perfusion rate.

The convective heat transfer term associated with blood flow is given by $q_b\ c_b(T - T_a)$ (q_b, organ perfusion rate per unit volume of tissue; c_b, specific heat of blood; T_a, arterial temperature; and T, local tissue temperature). The energy field in the perfused tissue domain is given by the bioheat transfer equation:

$$\rho_{tis} c_{tis} \frac{\partial T}{\partial t} = \mathcal{G}_{T_{tis}} \nabla^2 T + q_b c_b (T - T_a) + q_{met} + q_{so}, \quad (17)$$

where c_{tis} is the specific heat of the explored biological tissue, ρ_{tis} its density, $\mathcal{G}_{T_{tis}}$ its thermal conductivity, q_{met} the metabolic heat source (rate of energy deposition per unit volume assumed to be homogeneously distributed throughout the tissue of interest, but usually neglected), and q_{so} a possible heat source (e.g., in the case of thermal ablation).

This equation is coupled with the energy field equation in the flowing blood domain, which includes (1) a directional convective term due to the net flux of equilibrated blood $\rho_b c_b(\mathrm{v} \cdot \nabla T)$ (v, blood velocity, which can be composed of two terms, a hemodynamic and acoustic streaming component generated by mechanical effects of high-frequency focused ultrasound when this therapeutic procedure is used to destroy the tumor), (2) the contribution of the nearly equilibrated blood in a tissue temperature gradient $\mathcal{G}_{T_b} \nabla^2 T$ ($\mathcal{G}_{T_b}$, blood perfusion thermal conductivity), and (3) heat deposition q_h due to an imposed source:

$$\rho_b c_b \frac{\partial T}{\partial t} = \mathcal{G}_{T_b} \nabla^2 T + \rho_b c_b (\mathrm{v} \cdot \nabla T) + q_h. \quad (18)$$

Values of the thermal conductivity and diffusivity of cardiac and arterial walls are given in Tables 7 and 8.

The heat transfer coefficient for blood in a vessel (d, vessel bore; L, vessel length) can be evaluated from the Sieder–Tate equation, when $q_m c_p/(\mathcal{G}_T L) > 6$:

Table 7 Mean and standard deviation (SD) of thermal conductivity (mW/cm/C) and diffusivity ($\times 10^3$ cm^2/s) of aortas and atherosclerotic plaques at 35 °C (Source: Valvano)

Tissue	Thermal conductivity		Thermal diffusivity	
Normal aorta	4.76	0.41	1.27	0.07
Fatty plaque	4.84	0.44	1.28	0.05
Fibrous plaque	4.85	0.22	1.29	0.03
Calcified plaque	5.02	0.59	1.32	0.07

Table 8 Mean and standard deviation (SD) of thermal conductivity (mW/cm/K) and diffusivity ($\times 10^3$ cm^2/s) of myocardia at 37C (Source: Valvano)

Thermal conductivity		Thermal diffusivity	
Mean	SD	Mean	SD
5.31	0.37	1.61	0.20

$$h_T d/\mathcal{G}_T = 1.75\left(q_m c_p/(\mathcal{G}_T L)\right)^{0.33} \times \left(\mu_{pl}/\mu\right)^{0.14}, \quad (19)$$

where h_T is the heat transfer coefficient, c_p isobar heat capacity, $\mathcal{G}_T$ G_T the thermal conductivity, q_m the mass flow rate, and μ_{pl} the near-wall plasma viscosity at wall temperature.

Spatial variations in temperature distribution have been computed in a 3D muscle vascular model (Werner and Brinck 2001). The tissue domain is composed of a twin artery and vein, which give birth to dichotomic trees of arterioles and venules, with eight generations of paired, closely spaced vessels, assuming property constancy at each generation. The arteriovenous spacing, vessel bore and density, and flow rate depend on tissue depth. An efficiency function, which depends on the volumic tissue blood perfusion rate and radial coordinate, is proposed to improve the bioheat equation. Using an appropriate procedure to analyze Pennes data, the data support the theory (Wissler 1998); but the Pennes model, as in new bioheat transfer models, lacks experimental validation and reliable evaluation of tissue properties (Arkin et al. 1994).

Metabolic Blood Flow Regulation

Blood flow regulation is controlled by various local and remote mechanisms. Arterioles dilate or constrict in response to changing intravascular pressure (myogenic response), to mechanical stress via endothelial release of nitric oxide (mechanical stress-dependent response), to signal transmission both upstream and downstream along vessel walls (propagated or conducted response), and to local metabolism.

Oxygen exchange between blood and tissue cells occurs primarily in the microcirculation. In the microcirculation, blood flow is regulated by the local metabolic demand. Oxygen supply must match oxygen need. Regulatory messengers manufactured and released from a site of metabolic activity influence the tone of blood vessels. Active hyperemia is the increase in blood flow in regions where the metabolic activity rises.

Metabolic activity controls local blood flow via synthesized catabolites, such as CO_2; ADP; extracellular K^+ ions, particularly those released by contracting cardiac and skeletal muscles; hydrogen ion; and organic acids such as lactic acid, a carboxylic acid product of anaerobic metabolism generated from pyruvate by lactate dehydrogenase, and inorganic phosphate liberated by the hydrolysis of adenine nucleotides. These catabolites directly prime vasodilation of local arterioles, thus increasing blood flow. Other substances such as nitric oxide are involved in coupling metabolic demand to local and regional blood flows.

Metabolic blood flow regulation involves ATP release by red blood capsules that trigger arteriolar vasodilation. Red blood capsules respond to a lower oxygen level such as that happening during exercise by releasing ATP at a rate that depends on their oxyhemoglobin saturation level (Bergfeld and Forrester 1992). Secretion of ATP through SLC29a1 nucleoside transporter is electrically balanced by the simultaneous influx of extracellular chloride and/or bicarbonate across the erythrocyte membrane via SLC4a1 anion exchanger. Once released from RBCs, ATP binds to P2Y receptors on the luminal surface of the endothelium. Liberated ATP initiates a conducted response that triggers arteriolar vasodilation (McCullough et al. 1997; Arciero et al. 2008).

Autoregulation

The primary function of local blood flow control is the provision of an adequate supply of nutrients to match tissue activity, especially to maintain equilibrium between oxygen delivery and consumption. Blood flow distribution can be controlled by the central nervous system as well as locally, particularly in arterioles, independently of remote signaling (neural impulses and hormonal cues).

In 1902, W. Bayliss discovered that an elevated transmural pressure causes a paradoxical vasoconstriction and arterial resistance augmentation. This pressure-induced myogenic response is also called the Bayliss effect (Bayliss 1902).

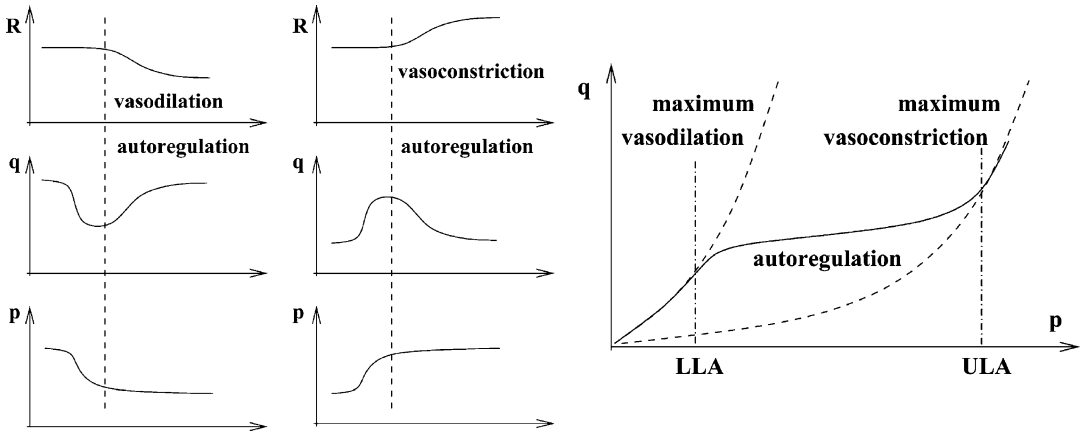

Fig. 4 Autoregulation of local blood flow. (*Left*) Perfusion of certain organs is autoregulated when the blood-driving pressure either decays or rises, the local blood flow being maintained almost constant by either vasodilation or vasoconstriction of the organ vasculature. (*Right*) Autoregulation occurs for a pressure range, between the lower (*LLA*) and upper limit of autoregulation (*ULA*)

The myogenic response is the mechanism of blood flow autoregulation that enables matching of blood supply to tissue nutrient and energy demand over a given pressure range (8–20 kPa [60–150 mmHg]).

The myogenic response, or myogenic autoregulation, is related to the intrinsic ability of resistance arteries to respond to a transmural pressure change, hence a type of mechanotransduction. Endoluminal pressure imposes a circumferential and axial stretch in the vessel wall and a shear stress at the wetted surface of the endothelium that are sensed by parietal cells. The myogenic response can change quantitatively (i.e., change in magnitude) and qualitatively (i.e., change in mediating mechanism) in response to environmental conditions.

Organ perfusion is autoregulated by blood-driving pressure variations. A nearly constant flow is maintained, although the blood pressure varies in a given range. The pressure–flow relation exhibits a very small slope (a quasi-plateau) in the autoregulatory range and steep slopes outside the autoregulatory range (Fig. 4).

An artery is maximally vasodilated below the lower limit and maximally vasoconstricted above the upper limit of autoregulation. Below the autoregulatory range, the pressure–flow relation of a given vessel matches the nonlinear pressure–flow curve of a maximally dilated vessel after vasodilator infusion into the explored organ, which disables autoregulation. The artery dilates with increasing pressure, hence reducing flow resistance and augmenting flow rate (Table 9). When the pressure rises beyond the autoregulatory range, the pressure–flow relation of the vessel follows the pressure–flow curve of a maximally constricted vessel.

Autoregulation thus fails whether the perfusion pressure is too low, dropping below the lower limit of autoregulation, local blood flow falling with decaying blood pressure, or too high, rising above the upper limit, the local blood flow heightening with elevating blood pressure.

Table 9 The vascular myogenic response refers to the intrinsic ability of a blood vessel to constrict in response to an increase in intraluminal pressure or dilate with a decrease in intraluminal pressure. Autoregulation aims at maintaining a constant blood flow rate (q) when the local pressure (p) changes. When the pressure decreases, a paradoxical vasodilation (VD) widens the local vessel caliber, hence reducing the local resistance ($R = \Delta p/q$), but potentiating the pressure drop. Conversely, when the pressure decreases, a paradoxical vasoconstriction (VC) narrows the vessel lumen, thereby elevating the local resistance, but strengthening the pressure rise

$\downarrow P \rightarrow VD \rightarrow \downarrow R \rightarrow q = \text{cst.}$
$\uparrow P \rightarrow VC \rightarrow \uparrow R \rightarrow q = \text{cst.}$

Autoregulation is aimed at ensuring an adequate blood flow and oxygen delivery to essential organs. The cerebral, cardiac, and renal circulation exhibit a strong autoregulation. The skeletal muscular and visceral circulation show a moderate autoregulation. The cutaneous circulation displays a slight autoregulation.

Autoregulation and Vascular Resistance

Autoregulation is based on modified vascular resistance, the ratio between perfusion pressure and blood flow:

$$R = \Delta p/q. \tag{20}$$

When blood pressure increases, stretched arteriole walls contract, their lumens narrow, and subsequently the local blood pressure further rises to maintain the blood flow rate at a nearly constant value. Usually, elevation in intracellular pressure in an elastic pipe leads to its expansion. Resistance blood vessels, small arteries and arterioles, thus behave oppositely. Vasoconstriction in autoregulatory segments of the arterial bed is aimed at keeping blood flow rate invariant. Conversely, when blood pressure decays, resulting vasodilation decreases vascular resistance; subsequently, the local blood pressure paradoxically declines, and the local blood flow remains almost constant.

The vascular myogenic response, an inherent property of smooth myocytes in walls of small arteries and arterioles, stabilizes not only the local blood flow rate but also the capillary filtration pressure when blood pressure changes.

Smooth muscle tone is controlled not only by hemodynamic stress applied by flowing blood to the vessel wall but also by metabolic and neural mechanisms. These control mechanisms are locally integrated (Davis 2012). The resulting vascular tone can thus be elevated or attenuated by nerve transmitters, autacoids, and hormones.

Table 10 Sensors and mechanotransduction mediators in the myogenic response (Source: Lidington et al. (2013); *ASIC* acid-sensing ion channel, *PKC* protein kinase-C, *PLA2* phospholipase A2, *PLC* phospholipase-C, *S1P* sphingosine-1-phosphate, *TREK* TWIK-related potassium channel, *TRP* transient receptor potential)

Function	Molecule types
Sensors	GPCRs
Transducers	TRPs, TREK1, ASIC2, Piezo-1/2
	Integrins
Messengers	S1P
Intracellular	PKC, Src, PLA2, PLC
Mediators	Vinculin, actin

Myogenic Signaling

The myogenic response (▶ Chap. 22, "Mechanotransduction and Vascular Resistance") relies on regulatory effectors of several signaling cascades that operate either in series or in parallel and cooperate or exert a mutual exclusion (Table 10) (Lidington et al. 2013): (1) sensors, such as stretch-sensitive G-protein-coupled receptors, stretch-activated cation channels, membrane-bound enzymes (e.g., MMP2 and MMP9), cell adhesion molecules such as integrins, and cytoskeleton and (2) cytosolic messengers that are either calcium-dependent (e.g., phospholipase-C and diacylglycerol, phospholipase-A2 and arachidonic acid metabolites, ryanodine-, and inositol trisphosphate-stimulated intracellular calcium release channels) or calcium-independent (e.g., protein kinase-C, RhoA GTPase, and RoCK kinase).

All myogenic mechanisms are potential contributors to the overall response with variable impact depending on the circumstances. Two organizational Ca^{2+}-dependent and Ca^{2+}-independent mechanisms are integrated and modulated Ca^{2+} concentration levels and sensitivity. Both the sensitivity to transmural pressure (i.e., the magnitude of the myogenic response) and the selection and weighting of contributors (i.e., the orchestration of calcium-dependent and calcium-independent signaling cascades that mediate the myogenic response) are under a temporal control.

The participation of various mechanisms can be modified, hence changing (Lidington et al. 2013) (1) the magnitude of the myogenic response with the recruitment of proximal vascular segments, dormant processes being activated, and/or (2) the pattern of the operating mode without necessary variation of the magnitude of the response.

Among mechanically activated proteins that initiate a signaling cascade, some sense directly the membrane stretch, and others are stimulated by a mediator downstream from force sensors. Nevertheless, both types are indiscriminately termed mechanosensitive. In any case, a mechanosensitive protein must react according to the application speed and amplitude of the mechanical stimulus. The activation time of mechanically stimulated proteins is very short: lower than 50 μs for membrane-tethered enzymes, than 5 ms for ion channels, and than 500 ms for G-protein activation (Storch et al. 2012). In addition, a given protein may not be mechanosensitive, but may react to mechanical cues in conjunction with other proteins within a macromolecular complex. In other words, mechanical signals can be sensed and transduced by mechanosensory protein complexes rather than a single molecule.

Arteriolar Network

Elements of an arteriolar tree may react sequentially, but independently, to changes in blood pressure to regulate capillary pressure (Davis 2012). Small reductions in perfusion pressure may provoke a dilation of the generation-1 arteriole, thereby preventing or minimizing downstream myogenic changes in the microcirculation. A sufficient perfusion pressure drop causes a maximal myogenic dilation of the parent arteriole. Any further decrease may cause myogenic dilation of generation-2 arterioles. Once these segments are maximally dilated, any further pressure decrease may be experienced by generation-3 arterioles and so on. Therefore, a progressive reduction in perfusion pressure may lead to sequential dilation of successive arteriolar generations. Axial progression of the myogenic response initiated upstream supports spreading of myogenic dilation or constriction from one generation to the next.

However, this process works only for certain vascular beds. The behavior of other microvascular circuits does not support the concept of a series-coupled myogenic effector with a vasodilation that progresses gently downstream, from parent to child arterioles. All arteriolar generations can dilate simultaneously. The smaller the arteriolar caliber, the higher the myogenic sensitivity, except in small arterioles with a discontinuous layer of smooth myocytes (Davis 2012). This feature hence explains the homogeneous pattern of dilation in response to progressive blood pressure reduction. Moreover, a third type of arteriolar network does not exhibit autoregulation.

High Intravascular Pressure

The mechanical stretch of the vascular wall acts as a stimulus on medial smooth myocytes to elicit myogenic contraction. Autoregulatory contraction of arterioles controls local blood flow in perfusion compartments.

In vivo, arteriolar blood pressure at rest, at least in rat cremaster muscle, is assessed to range from 9.3 to 10.6 kPa (Hill et al. 1992). In fact, an acute increase in intraluminal pressure from 4.0 to 5.3 kPa can prime vasoconstriction (Davis 2012).

This type of myogenic response may be antagonized by mechanical stress-dependent, endothelium-derived, and NO-induced vasodilation.

The myogenic behavior (myogenic vasoconstriction, maintenance of basal myogenic tone, and myogenic vasodilation) relies on mechanosensors in vascular smooth myocytes and subsequent transduction to adapt states of actin polymerization and contractility. Different mechanisms occur during initial and sustained phases of the myogenic response of rat small mesenteric arteries. Both phases depend on calcium influx through voltage-dependent calcium

channels (Chlopicki et al. 2001). However, only the sustained phase is mediated by a cytochrome-P450 ω-hydroxylase metabolite such as 20-hydroxyeicosatetraenoic acid and calcium-activated K^+ channel.

In fact, numerous signals participate in myogenic behavior, in addition to ion channels and cytosolic calcium (Zou et al. 2000), such as the RhoA–RoCK axis (Bolz et al. 2003), protein kinase-C (Yeon et al. 2002), and arachidonic acid derivatives (Frisbee et al. 2001). Epoxyeicosatrienoic acids are released from the endothelium in response to acetylcholine. They hyperpolarize smooth myocytes, open K_{Ca} channels, and relax arteries (Obara et al. 2002). Another major metabolite of arachidonic acid, 20-hydroxyeicosatetraenoic acid, is a potent vasoconstrictor. In normotensive salt-sensitive rats, myogenic activation of skeletal muscle resistance arteries does not depend on cytochrome-P450 ω-hydroxylase. On the other hand, in hypertensive salt-sensitive rats, myogenic activation of these vessels partly relies on 20HETE production, this substance inhibiting K_{Ca} channels via PKC, at least in canine basilar artery (Obara et al. 2002). Inhibition of the BK channel sensitizes the canine basilar artery to mechanical stretch.

Mechanotransduction in vascular smooth myocytes can result from myogenic, neurogenic, or hemodynamic stress or metabolic processes. The pathway starts at the plasma membrane and cell cortex to target the contractile cytoskeleton.

The myogenic contraction-triggering cascade relies on a connection between the extracellular matrix, cell adhesion sites, and cytoskeleton. The latter depends on integrins (Table 11) for both outside-in and inside-out signaling. Integrin mechanosensors are associated with the regulation of arteriolar caliber and hence vascular myogenic response, in addition to vascular permeability and remodeling (Martinez-Lemus et al. 2003).

Cell adhesion and corresponding forces result from interactions between fibronectin and α_5 β_1-integrin (Sun et al. 2005). Both α_5 β_1- and α_V β_3-integrins are needed for myogenic constriction (Martinez-Lemus et al. 2005). These integrins act as mechanosensors of vascular smooth myocytes that enable these cells to detect and respond to changes in intraluminal pressure.

Table 11 Integrins of vascular endothelial and smooth muscle cells (Source: Martinez-Lemus et al. (2003)). Cells of vascular walls connect their cytoskeleton to the extracellular matrix via integrins. The latter operate as assembly points for numerous cytoskeletal and signaling components. These cell surface receptors communicate with the extra- and intracellular media. They transmit forces from both sides and inside-out and outside-in signals used to control vascular tone, permeability, and wall remodeling. These mechanosensors decipher the pressure-dependent myogenic response and serve as detectors of certain molecules. Integrins of both cell types are enmeshed in a meshwork of interacting matrix proteins, such as collagen-1 and collagen-3 to collagen-6, elastin, several types of laminin, fibro- and vitronectin, osteopontin, tenascin, and thrombospondin. Integrins on vascular smooth myocytes and abluminal surface of endothelial cells participate in controlling vascular tone

Endothelial cell	Smooth myocyte
$\alpha_1\beta_1$	$\alpha_1\beta_1$
$\alpha_2\beta_1$	$\alpha_2\beta_1$
$\alpha_3\beta_1$	$\alpha_3\beta_1$
$\alpha_5\beta_1$	$\alpha_4\beta_1$
$\alpha_6\beta_1$	$\alpha_5\beta_1$
$\alpha_6\beta_4$	$\alpha_6\beta_1$
$\alpha_V\beta_3$	$\alpha_7\beta_1$
$\alpha_V\beta_5$	$\alpha_8\beta_1$
	$\alpha_9\beta_1$
	$\alpha_V\beta_1$
	$\alpha_V\beta_3$
	$\alpha_V\beta_4$
	$\alpha_V\beta_5$

Vascular smooth myocyte contraction is accompanied by a remodeling of both contractile and noncontractile components of the actin cytoskeleton and adhesion junctions. Integrin molecule reconfiguration and integrin population rearrangement contribute to reset arteriole reference state.

Numerous vascular integrins recognize the RGD matricryptic, integrin-binding motif of vascular wall matrix proteins such as collagen, fibronectin, and vitronectin. Matricryptic sites are active sites, such as Arg–Gly–Asp (RGD) and Leu–Asp–Val (LDV), which are hidden in the mature secreted form of matrix molecules. They become exposed upon conformational changes caused by oligomerization, adsorption, and

Table 12 Integrins on vascular myocytes and vascular tone. Once they are exposed to matricryptic site-containing peptides, for example, when a mechanical stress field is applied or upon matricryptin production, activated $\alpha_V\beta_3$-integrin inhibits the $Ca_V1.2b$ channel, thereby promoting vasodilation. On the other hand, $\alpha_4\beta_1$- and $\alpha_5\beta_1$-integrin support $Ca_V1.2b$ gating, via Src kinase and possibly protein kinase-A, which phosphorylate (activate) $Ca_V1.2b$ channel, thereby causing vasoconstriction in response to matricryptic site-containing peptides (Source: Martinez-Lemus et al. (2003))

Type	Effect (activatory matrix ligand)
$\alpha_4\beta_1$	Vasoconstriction
$\alpha_5\beta_1$	(Fibronectin)
	(Matricryptins)
$\alpha_V\beta_3$	Vasodilation
	(Vitronectin, fibronectin)
	(Matricryptins)

mechanical stress. Matricryptic sites contribute in particular to acute changes in vascular permeability. Matricryptins are active fragments of matrix molecules with exposed active matricryptic sites. They can bind to specific integrins and regulate arteriolar tone using calcium and potassium channels.

On endotheliocytes, $\alpha_5\beta_1$- and $\alpha_V\beta_3$-integrin respond to RGD matricryptic site-containing peptides and mechanical forces by launching production of vasoactive autacoids. On vascular myocytes, integrin-$\alpha_4\beta_1$ and integrin-$\alpha_5\beta_1$ cause vasoconstriction in response to LDV and RGD matricryptic site-containing peptides, respectively, whereas integrin-$\alpha_V\beta_3$ provokes vasodilation in response to RGD matricryptic site-containing peptides (Table 12) (Martinez-Lemus et al. 2003).

Some synthetic peptides containing the RGD integrin-binding sequence repress spontaneous myogenic tone in isolated arterioles via $\alpha_V\beta_3$-integrin. On the other hand, activated $\alpha_4\beta_1$- and $\alpha_5\beta_1$-integrin support myogenic tone. Certain RGD-containing peptides can attenuate the myogenic response to step increase in intravascular pressure (Martinez-Lemus et al. 2003).

In addition, shear-mediated endothelial cell response is triggered upon activation of integrins and inwardly rectifying $K_{IR}2.1$ channel within seconds, thereby causing endothelial cell hyperpolarization. The signaling cascade includes the integrin–SHC connection; activation of FAK, JNK, ERK1, and ERK2 kinases, as well as that of SREBP1 and Jun factors; and modulation of Rho activity (Martinez-Lemus et al. 2003).

Moreover, in cooperation with connexins, integrins may contribute to signal propagation that enables remote regulation of resistive vessels. A local stimulation of integrins can actually initiate a remote change in vascular caliber. Last, but not least, upon interaction with their ligands, integrins can operate via the calcium channel and cytosolic influx in both endothelial and smooth muscle cells.

Mechanics of the fibronectin–integrin–actomyosin cytoskeleton complex can be modulated by G-protein-coupled receptors. Stimulated G-protein-coupled receptors change the cortical elasticity as well as cell adhesion strength (Hong et al. 2012). Vascular smooth myocyte relaxation reduces coupling to extracellular matrix proteins, whereas contraction elicits a tight coupling. Integrin-mediated adhesion of vascular smooth myocytes to the extracellular matrix is reinforced during contraction and attenuated during relaxation. A vasodilator (e.g., adenosine) softens the plasma membrane–cytoskeleton complex and reduces the membrane adhesion strength. On the other hand, a vasoconstrictor (e.g., angiotensin-2) stiffens the complex and heightens the membrane adhesion strength.

Cortical stiffness can result from rearrangement and cross linking of the actin mesh, generation of actin bundles (actin stress fibers), actin binding to integrins, interaction of actin with cortical myosin, creation of new actin fibers, and stretch of cortical actin by connected actin of the contractile compartment (Schmid-Schönbein 2012).

Low Intravascular Pressure

Vasodilation can result from hyperpolarization generated by activity of endothelial Ca^{2+}-activated K^+ channels $K_{Ca}2.3$ (SK or SK_{Ca}) and $K_{Ca}3.1$ (IK or IK_{Ca}), among other mechanisms such as vasodilation dependent on nitric oxide or prostacyclin.

This hyperpolarization, the predominant endothelium-dependent mechanism in small resistive arteries and arterioles, spreads both radially and longitudinally. It is transmitted to adjacent smooth myocytes via endothelial projections through the basement membrane and internal elastic lamella toward smooth myocytes. Calcium-activated K^+ channels localize to myoendothelial microdomains between endothelial and adjoining smooth muscle cells.

These two cell types generate elementary and spatially restricted Ca^{2+} events spontaneously. In particular, spontaneous, rapid, localized (subcellular) Ca^{2+} sparks through activated ryanodine-sensitive calcium channels on the sarcoplasmic reticulum of cerebral artery myocytes attenuate the vascular tone, as they activate BK channels (Nelson et al. 1995). The latter hyperpolarize and dilate pressurized arteries.

In fact, three types of nanodomains on projections can be defined: (1) myoendothelial gap junction that facilitates the intercellular transfer of ions (e.g., Ca^{2+}) and small molecules (e.g., inositol trisphosphate [IP_3]) and (2) cluster of K_{Ca} channels and (3) nonselective cation transient receptor potential (TRP) channels. The 2 latter nanodomains can merge.

An intercellular functional unit is composed of (1) connexins that form gap junctions, (2) endothelial IP_3 receptor (IP_3R) and $K_{Ca}3.1$ channel, and (3) inward rectifier $K_{IR}2.1$ channel and voltage-dependent $Ca_V1.2$ channel on smooth myocyte.

In particular, Ca^{2+} ion can also be locally released through IP_3 receptors of endothelial endoplasmic reticulum to create spontaneous, localized, and asynchronous calcium pulsars in myoendothelial junctions. Calcium pulsars encode signals between vascular endothelial and smooth muscle cells. They differ from Ca^{2+} sparks generated by ryanodine receptors. One target of calcium pulsars is the $K_{Ca}3.1$ channel in endothelial projections to relax the adjoining smooth myocyte. Exiting K^+ ion targets the myocyte $K_{IR}2.1$ channel to trigger hyperpolarization of the myocyte plasma membrane.

Endothelial, mechanosensitive TRPV4 channels cluster on the myoendothelial junction. They are selectively activated at low intravascular pressure (Bagher et al. 2012). Intraluminal pressure below 6.7 kPa causes TRPV4 channel opening and two- to three-fold increase in the frequency of endothelial Ca^{2+} sparklets. These localized Ca^{2+} sparklets on the endothelial plasma membrane activate endothelial IK, but not SK channels. In addition, Ca^{2+} sparklets may enhance the frequency of Ca^{2+} puff and pulsar, as Ca^{2+} can stimulate clustered IP_3Rs on the myoendothelial junction.

Cerebral Arterioles

The pressure-dependent activation of vascular smooth myocytes of cerebral arterioles is the main regulator of blood flow in the brain. The greater the wall stretch is, the stronger the vasoconstriction.

Increased vessel wall stretch caused by rising perfusion pressure activates phospholipase-C that produces, via cytochrome-P450-4A, 20-hydroxyeicosatetraenoic acid, which in turn, activates protein kinase-C (Harder et al. 1998). Protein kinase-C inhibits potassium channels, especially calcium-activated potassium channels, modifying the membrane potential of the smooth myocytes and inducing vasoconstriction.

The metabolic activity of the nerve cells also intervenes. Glutamic acid is released from metabolically active neurons, stimulating astrocytes for arachidonic acid production. Arachidonic acid is converted by cytochrome-P450-2C11 to epoxyeicosatrienoic acid, which stimulates calcium-activated potassium channels, antagonizing 20-hydroxyeicosatetraenoic acid. Cerebral autoregulation thus results from a balance between vasoconstriction generated by 20-hydroxyeicosatetraenoic acid and vasodilation induced by epoxyeicosatrienoic acid. Astrocytes also release other vasoactive molecules, such as thromboxane-A2, prostacyclin, and prostaglandin-E and prostaglandin-F. The calcium-activated potassium channels can be affected by various mediators (nitric oxide, adenosine, and prostacyclin).

Renal Arterioles

Renal autoregulation is mainly located in glomerular arterioles. Stretch-activated vasoconstriction and tubuloglomerular feedback maintain a nearly constant blood flow. The tubuloglomerular negative feedback deals with increased delivery of water and salts to the distal tubule, which causes vasoconstriction. This feedback can be affected by angiotensin-2, nitric oxide, thromboxane, 20-hydroxyeicosatetraenoic acid, and adenosine triphosphate.

Coronary Arterioles

Coronary blood flow is tightly coupled with oxygen demand, as myocardium has a very high basal oxygen consumption. Increased cardiac activity augments coronary blood flow. Coronary autoregulation works for perfusion pressures between 8 and 26 kPa.

Coronary circulation produces vasoactive substances. Endothelial production of nitric oxide mediates coronary vasodilation. Coronary endothelial cells can also produce epoxyeicosatrienoic acids, which cause coronary vasodilation. In addition, ATP-gated potassium channels and adenosine are implicated.

Ischemic myocardium releases increased amounts of adenosine, which regulates coronary flow. Oxygen is a major mediator. Myocardial oxygen consumption increases when coronary blood flow augments, antagonizing autoregulation. In abnormal states, coronary autoregulation can change. Hypoperfused human epicardial coronary arteries change their autoregulatory responsiveness. Vasoconstriction distal to the site of coronary angioplasty results from altered autoregulation (Fischell et al. 1990).

Role of Vascular Smooth Myocytes

Autoregulation is mediated by vascular smooth myocytes independently of endothelial cells. Vasoconstriction that results from an increase in pressure inside most small resistance arteries involves stretch-induced activation of plasmalemmal, nonselective cation channels of vascular smooth myocytes. This activation causes membrane depolarization, calcium influx through $Ca_V1.2$ channels, and smooth muscle contraction (Davis and Hill 1999).

Stretch-induced channel activity originates from interaction between mechanosensitive angiotensin Gq-coupled AT_2 receptor and cation TRPC6 channel (Mederos et al. 2008). The former can be activated by membrane stretch in the absence of its ligand (Zou et al. 2004). Excited Gq protein activates phospholipase-C that hydrolyzes the membrane phospholipid phosphatidylinositol (4,5)-bisphosphate into diacylglycerol and inositol trisphosphate. Diacylglycerol stimulates several members of the TRP family, such as TRPC3, TRPC6, and TRPC7 (Hofmann et al. 1999). In fact, PIP_2, DAG, and IP_3 are all able to prime activity of certain TRP channels (Nilius et al. 2007).

Blood Flow Modeling in Arterioles

Some mathematical models of blood flow regulation describe the mechanics of the vascular wall exposed to a pressure field and its reaction by varying the vessel tone. The model of thin-walled, elastic, cylindrical vessels is based on Laplace's law, this hypothesis being valid for a ratio of a wall thickness to hydraulic diameter much smaller than 1. Simple constitutive laws relate wall shear stress to vessel wall tension.

Changes in hematocrit (Ht) influence blood pressure. A small hematocrit elevation is associated with decreased blood pressure and increased blood flow rate. Augmented hematocrit and resulting rise of blood viscosity heighten wall shear stress (WSS), thereby increasing nitric oxide production in the endothelium and subsequently causing vasodilation resulting from stress-induced nitric oxide release from the endothelium.

Arteriolar mechanics, which is responsible for autoregulation of blood flow, was modeled incorporating elastic (passive) and myogenic (active) responses modulated by wall shear stress effect

for small changes in luminal pressure (p_i) and hematocrit (Sriram et al. 2012). This model considers a one-dimensional, steady, laminar, fully developed flow (Poiseuille flow) in a thick-walled, elastic, cylindrical arteriole (straight duct of circular cross section; unstressed internal radius $R_i = 10$ µm, endothelial thickness 1 m, and wall thickness 10 m). Wall shear stress is given by $c_w = (\Delta p_i/L)R_i/2$ and the volumetric flow rate by

$$q = \frac{\pi R_i^4 \Delta p_i}{8\mu_{\mathrm{pl}}}\left(1 + \lambda_{co}^4\left[\frac{\mu_{\mathrm{pl}}}{\mu_{\mathrm{co}}} - 1\right]\right), \tag{21}$$

where μ_{co} and μ_{pl} are the blood core and plasma layer viscosity, respectively.

The 2-layer blood domain in the arteriolar lumen consists of a cell-rich core and a plasma layer. The thickness of the plasma layer is assumed to be related to Ht by the following linear relation:

$$h_{\mathrm{pl}} = \kappa_1 Ht + \kappa_2, \tag{22}$$

κ_3 and κ_4 being fitting parameters. Then, the normalized thicknesses of blood core (λ_{co}) and plasma layer (λ_{pl}) in an arteriole are given by

$$\lambda_{\mathrm{pl}} - h_{\mathrm{pl}}/R; \quad \lambda_{\mathrm{co}} = 1 - \lambda_{\mathrm{pl}}.$$

The blood core viscosity (μ_{co}) is related to the blood core Ht (Ht_{co}) by another linear relation:

$$\mu_{\mathrm{co}} = \kappa_3 Ht_{\mathrm{co}} + \kappa_4, \tag{23}$$

where κ_3 and κ_4 are fitting parameters ($\kappa_3 = 1.68 \times 10^{-4}$ and $\kappa_4 = 43.48 \times 10^{-4}$ Pl). The core hematocrit is related to the measured Ht by

$$Ht = 2Ht_{\mathrm{co}}\lambda_{\mathrm{co}}^2\left(1 - \lambda_{\mathrm{co}}^2 + \lambda_{\mathrm{co}}^2\frac{\mu_{\mathrm{pl}}}{2\mu_{\mathrm{co}}}\right) \times \left(1 - \lambda_{\mathrm{co}}^2 + \lambda_{\mathrm{co}}^2\frac{\mu_{\mathrm{pl}}}{\mu_{\mathrm{co}}}\right)^{-1}. \tag{24}$$

The blood vessel is supposed to be a tethered cylinder; axial strain is neglected and the relation between radial strain (e_r) and radial (c_r) and circumferential (c_θ) stress vector is assumed to be linear:

$$e_r = \frac{r}{R_i}\left[c_\theta\left(1 - \nu_P^2\right) - \nu_P c_r(1 + \nu_P)\right], \tag{25}$$

where $E = 1 \times 10^4$ N/m^2 is the elastic modulus of blood vessel supposed to be constant and $\nu_P = 0.5$ the Poisson ratio (incompressible material).

The active (myogenic) and passive responses of vessel wall to blood flow are the sums of their respective passive $\left(c_r^P\right)$ and $\left(c_\theta^P\right)$ and active $\left(c_r^a\right)$ and $\left(c_\theta^a\right)$ components. The passive components are derived from Lame's equations:

$$\begin{aligned} c_r^P &= \frac{R_i^2 p_i}{R_e^2 - R_i^2}\left(1 - \frac{R_e^2}{r^2}\right); \\ c_\theta^P &= \frac{R_i^2 p_i}{R_e^2 - R_i^2}\left(1 + \frac{R_e^2}{r^2}\right). \end{aligned} \tag{26}$$

The active components are assumed to be linearly proportional to the tension at the surface of the vessel wall ($p_i R_i/2$), that is, the myogenic response is a simple function of wall tension:

$$\begin{aligned} c_r^a &= \frac{R_i^2}{R_e^2 - R_i^2}\left(1 - \frac{R_e^2}{r^2}\right)\gamma wss k_5 p_i \frac{R_i}{R_{\mathrm{ref}}}; \\ c_\theta^a &= \frac{R_i^2}{R_e^2 - R_i^2}\left(1 + \frac{R_e^2}{r^2}\right)\gamma wss k_5 p_i \frac{R_i}{R_{\mathrm{ref}}}, \end{aligned} \tag{27}$$

where $\gamma wss = -\tanh(\kappa_6/c_w)$ is the modulation of the myogenic response by the wall shear stress normalized with a fitting parameter (κ_6), R_{ref} the vessel radius at baseline pressure, and $\kappa_5 = 8$ another fitting parameter using experimental observations.

The maximum NO synthesis rate ($p_{NOmax} = 150$ µmol/s) is supposed to evolve linearly with the wall shear stress. Nitric oxide production follows Michaelis–Menten kinetics (with Michaelis–Menten constant $K_M = 4.7$); hence, the corresponding reaction rate $\mathcal{R}$ is given by

$$\mathcal{R} = \frac{P_{N_{max}} p_{O_2}}{p_{O_2} + K_M}, \tag{28}$$

where p_{O2} is the oxygen partial pressure.

In the cell-rich core, NO concentration (c_{NO}) is governed by the following steady-state reaction–diffusion equation:

$$\frac{\mathcal{D}_{NO_f}}{r}\frac{\partial}{\partial r}\left(r\frac{\partial c_{NO}}{\partial r}\right) = d_f c_{NO}, \qquad (29)$$

where $\mathcal{D}_{NO_f} = 3{,}300\ m^2/s$ is the diffusion coefficient of NO in the cell-rich core and $d_f = 382.5/s$ the scavenging rate of NO by red blood capsules, which can be assumed to remain constant, whatever the hematocrit.

In the plasma layer and glycocalyx (subscript f), the transport of NO and O_2 is assumed to satisfy the following steady-state diffusion equations:

$$\frac{\mathcal{D}_{NO_f}}{r}\frac{\partial}{\partial r}\left(r\frac{\partial c_{NO}}{\partial r}\right) = 0, \qquad (30)$$

$$\frac{s_{O_2}\mathcal{D}_{O_{2_f}}}{r}\frac{\partial}{\partial r}\left(r\frac{\partial p_{O_2}}{\partial r}\right) = 0, \qquad (31)$$

where $s_{O2} = 0.01\ \mu mol/Pa$ is the solubility of O_2 in the fluid phase and $\mathcal{D}_{O_{2_f}} = 2,800\ \mu m^2/s$ is the diffusivity of O_2 in the vessel lumen.

In the endothelium (subscript w), the rate of O_2 consumption is assumed to be twice the rate of NO production. The transport equations become

$$\frac{\mathcal{D}_{NO_w}}{r}\frac{\partial}{\partial r}\left(r\frac{\partial c_{NO}}{\partial r}\right) + \mathcal{R} = 0, \qquad (32)$$

and

$$\frac{So_2\mathcal{D}o2_w}{r}\frac{\partial}{\partial r}\left(r\frac{\partial po_2}{\partial r}\right) - 2\mathcal{R} = 0 \qquad (33)$$

where $\mathcal{D}_{NO_w}$ and $\mathcal{D}_{O_{2_w}}$ are the diffusivities of NO and O_2 in the arteriolar wall.

In the remaining part of the arteriolar wall,

$$\frac{\mathcal{D}_{NO_w}}{r}\frac{\partial}{\partial r}\left(r\frac{\partial c_{NO}}{\partial r}\right) - dw c_{NO} = 0, \qquad (34)$$

and

$$\frac{So_2\mathcal{D}o_{2_w}}{r}\frac{\partial}{\partial r}\left(r\frac{\partial p_{o_2}}{\partial r}\right) - \mathcal{R} = 0, \qquad (35)$$

where $d_w = 1/s$ is the rate of consumption of NO in the arteriolar wall.

The steady blood flow rate through a single arteriole was thus shown to depend on NO production and availability and the balance between passive and active (myogenic) mechanical responses of the arteriole wall. Transient effects in both the viscoelastic response of the arteriole wall and NO production as well as wall anisotropy were neglected, but these hypotheses should not change the conclusion.

Summary and Concluding Remarks

The microcirculatory compartment is a major regulator of the internal milieu of the body's tissue. Approximatively 10 % of circulating blood reside in capillaries (about 7 % in the heart, 15 % in arteries, and 68 % in veins). Microcirculation is responsible for exchange of gas, nutrients, and wastes between blood and perfused tissues. Functional hyperemia is the increase in blood flow triggered by the cellular activity.

Via its microcirculation, the digestive tract delivers nutrients to blood. Similarly, the detoxification (liver) and excretory system (biliary circuit, kidney and urinary tract, large intestine, lung for gaseous wastes, and sweat glands) removes wastes. The respiratory tract with its set of alveolocapillary membranes supplies oxygen to blood and exhales carbon dioxide.

Homeostasis is the dynamical process that maintains the relative constancy of the internal milieu, more precisely, that enables fluctuations of a physiological quantity in a narrow range centered on a set point. The internal milieu refers to a set of physiological variables that ensure a proper framework for cell fate and metabolism, such as body temperature, blood volume and pressure, and concentrations of molecules carried by blood, among others.

Homeostasis relies on three elements: (1) a sensor that detects a change in external and/or internal factors and (2) an integrator that compares the detected change, compares to the corresponding set point, and signals to (3) effectors that correct the environmental change using fast and slow compensatory mechanisms.

The hypothalamus and circumventricular organs are detectors and integrators that regulate the body's temperature, blood pressure, breathing rate, blood pH, and glycemia as well as concentration of other blood molecules, among other tasks. The hypothalamus controls the activity of the medulla oblongata and endocrine glands via release-stimulating and release-inhibiting hormones.

The body's homeostasis relies on short-, medium-, and long-term reactions. The short-term regulation comprises the control of the cardiac function and vasomotor tone.

The medium-term regulation involved the neuroendocrine system. The endocrine system encompasses mainly both the cortex and medulla of adrenal glands, thyroid, and sexual organs (and, to a lesser extent, kidney, heart, adipose tissue, bone marrow, parathyroid, liver, and digestive tract). It is influenced by the hypothalamo-pituitary axis. The central integrator includes hypothalamus, pineal body (or epiphysis), and pituitary gland (or hypophysis) with its anterior (adenohypophysis) and posterior (neurohypophysis) lobes.

The long-term regulation is carried out by kidneys that secrete some hormones, such as renin, erythropoietin, thrombopoietin, and calcitriol, on the one hand, and govern excretion or reabsorption of sodium and water, on the other. The renin–angiotensin axis primes arterial constriction and increases blood volume via vasopressin and aldosterone, thereby raising blood pressure.

A feedback enables maintenance of homeostasis. The vasomotor center raises blood pressure, but once the correction has been achieved, the center stops to signal.

Oxygen transport in the microvasculature depends on (1) the blood O_2 content, that is, the O_2 partial pressure and blood O_2-carrying capacity, that is, O_2-hemoglobin saturation, (2) local blood flow rate, (3) blood–tissue transfer conditions, (4) kinetics of O_2 release from hemoglobin, and (5) tissular O_2 consumption.

As oxygen diffuses already in tissues from precapillary arterioles, the O_2 partial pressure is lower in capillaries and arterioles operate in gas exchange.

Countercurrent transfer between paired arteriole and venule running side by side close to each other increases venular O_2 content. Therefore, venules can also participate in mass transfer.

Ischemia can be associated with leukocyte aggregation to walls of venules and small arteries. Leukocyte aggregation can reversibly cause local, complete, vascular occlusion. Restoration of blood flow supported by a reactive hyperemia requires degradation of these leukocyte clusters. Stimulatory drugs are aimed at improving the microcirculatory hemodynamics and blood and lymph rheology.

References

Agre P, Brown D, Nielsen S (1995) Aquaporin water channels: unanswered questions and unresolved controversies. Curr Opin Cell Biol 7:472–483

Anderson JL, Malone DM (1974) Mechanism of osmotic flow in porous membranes. Biophys J 14:957–982

Arciero JC, Carlson BE, Secomb TW (2008) Theoretical model of metabolic blood flow regulation: roles of ATP release by red blood cells and conducted responses. Am J Physiol Heart Circ Physiol 295: H1562–H1571

Aris R (1956) On the dispersion of a solute in a fluid through a tube. Proc R Soc Lond A Math Phys Sci 235:67–77

Arkin H, Xu LX, Holmes KR (1994) Recent developments in modeling heat transfer in blood perfused tissues. IEEE T Bio-Med Eng 41:97–107

Armulik A, Genové G, Mäe M, Nisancioglu MH, Wallgard E, Niaudet C, He L, Norlin J, Lindblom P, Strittmatter K, Johansson BR, Betsholtz C (2010) Pericytes regulate the blood–brain barrier. Nature 468:557–561

Bagher P, Beleznai T, Kansui Y, Mitchell R, Garland CJ, Dora KA (2012) Low intravascular pressure activates endothelial cell TRPV4 channels, local Ca^{2+} events, and IKCa channels, reducing arteriolar tone. Proc Natl Acad Sci U S A 109:18174–18179

Barman SA, Taylor AE (1990) Effect of pulmonary venous pressure elevation on vascular resistance and compliance. Am J Physiol Heart Circ Physiol 258: H1164–H1170

Bates DO (2010) Vascular endothelial growth factors and vascular permeability. Cardiovasc Res 87:262–271

Bayliss W (1902) On the local reactions of the arterial wall to changes of internal pressure. J Physiol 28:220–231

Beard DA, Bassingthwaighte JB (2000) Advection and diffusion of substances in biological tissues with complex vascular networks. Ann Biomed Eng 28:253–268

Bergfeld GR, Forrester T (1992) Release of ATP from human erythrocytes in response to a brief period of hypoxia and hypercapnia. Cardiovasc Res 26:40–47

Bolz SS, Vogel L, Sollinger D, Derwand R, Boer C, Pitson SM, Spiegel S, Pohl U (2003) Sphingosine kinase modulates microvascular tone and myogenic responses through activation of RhoA/Rho kinase. Circulation 108:342–347

Caro CG, Nerem RM (1973) Transport of C4-cholesterol between serum and wall in perfused dog common carotid artery. Circ Res 32:187–205

Caro CG, Lever MJ, Laver-Rudich Z, Meyer F, Liron N, Ebel W, Parker KH, Winlove CP (1980) Net albumin transport across the wall of the rabbit common carotid artery perfused in situ. Atherosclerosis 37:497–511

Chen SC, Liu KM, Wagner RC (1998) Three-dimensional analysis of vacuoles and surface invaginations of capillary endothelia in the eel rete mirabile. Anat Rec 252:546–553

Chlopicki S, Nilsson H, Mulvany MJ (2001) Initial and sustained phases of myogenic response of rat mesenteric small arteries. Am J Physiol Heart Circ Physiol 281:H2176–H2183

Cohn HI, Harris DM, Pesant S, Pfeiffer M, Zhou RH, Koch WJ, Dorn GW 2nd, Eckhart AD (2008) Inhibition of vascular smooth muscle G protein-coupled receptor kinase 2 enhances alpha1D-adrenergic receptor constriction. Am J Physiol Heart Circ Physiol 295: H1695–H1704

Coomber BL, Stewart PA (1985) Morphometric analysis of CNS microvascular endothelium. Microvasc Res 30:99–115

Curry FE (1984) Mechanism and thermodynamics of transcapillary exchange. In: Renkin EM, Michel CC (eds) Microcirculation, handbook of physiology. The Cardiovascular System, American Physiological Society, Bethesda

Curry FRE, Adamson RH (2010) Vascular permeability modulation at the cell, microvessel, or whole organ level: towards closing gaps in our knowledge. Cardiovasc Res 87:218–229

Curry FRE, Noll T (2010) Spotlight on microvascular permeability. Cardiovasc Res 87:195–197

Daneman R, Zhou L, Kebede AA, Barres BA (2010) Pericytes are required for blood- brain barrier integrity during embryogenesis. Nature 468:562–566

Davis MJ (2012) Perspective: physiological role(s) of the vascular myogenic response. Microcirculation 19:99–114

Davis MJ, Hill MA (1999) Signaling mechanisms underlying the vascular myogenic response. Physiol Rev 79:387–423

Dawson CA, Rickaby DA, Linehan JH (1986) Location and mechanisms of pulmonary vascular volume changes. J Appl Physiol 60:402–409

Desjardins C, Duling BR (1990) Heparinase treatment suggests a role for the endothelial cell glycocalyx in regulation of capillary hematocrit. Am J Physiol Heart Circ Physiol 258:647–654

Durán WN, Breslin JW, Sánchez FA (2010) The NO cascade, eNOS location, and microvascular permeability. Cardiovasc Res 87:254–261

Ethier CR (2002) Computational modeling of mass transfer and links to atherosclerosis. Ann Biomed Eng 30:461–471

Fahraeus R, Lindqvist T (1931) The viscosity of the blood in narrow capillary tubes. Am J Physiol 96:562–568

Feng J, Weinbaum S (2000) Lubrication theory in highly compressible porous media: the mechanics of skiing, from red cells to humans. J Fluid Mech 422:281–317

Fischell TA, Bausback KN, McDonald TV (1990) Evidence for altered epicardial coronary artery autoregulation as a cause of distal coronary vasoconstriction after successful percutaneous transluminal coronary angioplasty. J Clin Invest 86:575–584

Frisbee JC, Roman RJ, Krishna UM, Falck JR, Lombard JH (2001) 20-HETE modulates myogenic response of skeletal muscle resistance arteries from hypertensive Dahl-SS rats. Am J Physiol Heart Circ Physiol 280: H1066–H1074

Fry DL (1987) Mass transport, atherogenesis, and risk. Arteriosclerosis 7:88–100

Garon A, Jullien S, Manseau J (2001) Numerical simulation of local mass transfer from an endovascular device. In: ASME-AIChE-AIAA 35th national heat transfer conference, Anaheim

Grant J (2004) Modélisation du transport de macromolécules à travers la paroi artérielle (Modeling of the macromolecule transport through the arterial wall). MSc thesis, Ecole Polytechnique de Montréal

Hanson WL, Emhardt JD, Bartek JP, Latham LP, Checkley LL, Capen RL, Wagner WW (1989) Site of recruitment in the pulmonary microcirculation. J Appl Physiol 66:2079–2083

Harder DR, Roman RJ, Gebremedhin D, Birks EK, Lange AR (1998) A common pathway for regulation of nutritive blood flow to the brain: arterial muscle membrane potential and cytochrome P450 metabolites. Acta Physiol Scand 164:527–532

He P (2010) Leucocyte/endothelium interactions and microvessel permeability: coupled or uncoupled? Cardiovasc Res 87:281–290

Hill MA, Trippe KM, Li QX, Meininger GA (1992) Arteriolar arcades and pressure distribution in

cremaster muscle microcirculation. Microvasc Res 44:117–124
Hofmann T, Obukhov AG, Schaefer M, Harteneck C, Gudermann T, Schultz G (1999) Direct activation of human TRPC6 and TRPC3 channels by diacylglycerol. Nature 397:259–263
Hong Z, Sun Z, Li Z, Mesquitta WT, Trzeciakowski JP, Meininger GA (2012) Coordination of fibronectin adhesion with contraction and relaxation in microvascular smooth muscle. Cardiovasc Res 96:73–80
Huang ZJ, Tarbell JM (1997) Numerical simulation of mass transfer in porous media of blood vessel walls. Am J Physiol Heart Circ Physiol 273:464–477
Huang Y, Rumschitzki D, Chien S, Weinbaum S (1994) A fiber matrix model for the growth of macromolecule leakage spots in the arterial intima. J Biomech Eng 116:430–445
Jäger W, Mikelić A (2000) On the interface boundary conditions by Beavers, Joseph and Saffman. SIAM J Appl Math 60:1111–1127
Kaazempur-Mofrad MR, Ethier CR (2001) Mass transport in an anatomically realistic human right coronary artery. Ann Biomed Eng 29:121–127
Levick JR, Michel CC (2010) Microvascular fluid exchange and the revised Starling principle. Cardiovasc Res 87:198–210
Lidington D, Schubert R, Bolz SS (2013) Capitalizing on diversity: an integrative approach towards the multiplicity of cellular mechanisms underlying myogenic responsiveness. Cardiovasc Res 97:404–412
Manseau J (2002) Étude numérique d'un modèle de transport de macromolécules à travers la paroi artérielle (Numerical study of a macromolecule transport model through the arterial wall). MSc thesis, Ecole Polytechnique de Montréal
Martinez-Lemus LA, Wu X, Wilson E, Hill MA, Davis GE, Davis MJ, Meininger GA (2003) Integrins as unique receptors for vascular control. J Vasc Res 40:211–233
Martinez-Lemus LA, Crow T, Davis MJ, Meininger GA (2005) αV β3- and α5 β1-integrin blockade inhibits myogenic constriction of skeletal muscle resistance arterioles. Am J Physiol Heart Circ Physiol 289: H322–H329
McCullough WT, Collins DM, Ellsworth ML (1997) Arteriolar responses to extracellular ATP in striated muscle. Am J Physiol Heart Circ Physiol 272:H1886–H1891
Mederos y, Schnitzler M, Storch U, Meibers S, Nurwakagari P, Breit A, Essin K, Gollasch M, Gudermann T (2008) Gq-coupled receptors as mechanosensors mediating myogenic vasoconstriction. EMBO J 27:3092–3103
Michel CC, Curry FE (1999) Microvascular permeability. Physiol Rev 79:703–761
Moore JA, Ethier CR (1997) Oxygen mass transfer calculations in large arteries. J Biomech Eng 119:469–475
Nelson MT, Cheng H, Rubart M, Santana LF, Bonev AD, Knot HJ, Lederer WJ (1995) Relaxation of arterial smooth muscle by calcium sparks. Science 270:633–637
Ngok SP, Geyer R, Liu M, Kourtidis A, Agrawal S, Wu C, Seerapu HR, Lewis-Tuffn LJ, Moodie KL, Huveldt D, Marx R, Baraban JM, Storz P, Horowitz A, Anastasiadis PZ (2012) VEGF and Angiopoietin-1 exert opposing effects on cell junctions by regulating the Rho GEF Syx. J Cell Biol 199:1103–1115
Nilius B, Owsianik G, Voets T, Peters JA (2007) Transient receptor potential cation channels in disease. Physiol Rev 87:165–217
Obara K, Koide M, Nakayama K (2002) 20-Hydroxyeicosatetraenoic acid potentiates stretch-induced contraction of canine basilar artery via PKC alpha-mediated inhibition of KCa channel. Br J Pharmacol 137:1362–1370
Oldendorf WH, Cornford ME, Brown WJ (1977) The large apparent work capability of the blood–brain barrier: a study of the mitochondrial content of capillary endothelial cells in brain and other tissues of the rat. Ann Neurol 1:409–417
Pennes HH (1948) Analysis of tissue and arterial blood temperatures in the resting human forearm. J Appl Physiol 1:93–122
Peppiatt CM, Howarth C, Mobbs P, Attwell D (2006) Bidirectional control of CNS capillary diameter by pericytes. Nature 443:700–704
Perktold K, Prosi M, Zunino P (2009) Mathematical models of mass transfer in the vascular walls (Chap. 7). In: Formaggia L, Quarteroni A, Veneziani A (eds) Cardiovascular mathematics: modeling and simulation of the circulatory system. Springer, Milano
Pries AR, Secomb TW, Jacobs H, Sperandio M, Osterloh K, Gaehtgens P (1997) Microvascular blood flow resistance: role of endothelial surface layer. Am J Physiol Heart Circ Physiol 273:2272–2279
Prosi M, Zunino P, Perktold K, Quarteroni A (2005) Mathematical and numerical models for transfer of low density lipoproteins through the arterial walls: a new methodology for the model set up with applications to the study of disturbed lumenal flow. J Biomech 38:903–917
Quarteroni A, Veneziani A, Zunino P (2002a) Mathematical and numerical modeling of solute dynamics in blood flow and arterial walls. SIAM J Numer Anal 39:1488–1511
Quarteroni A, Veneziani A, Zunino P (2002b) A domain decomposition method for advection–diffusion processes with application to blood solutes. SIAM J Sci Comput 23:1959–1980
Rabiet MJ, Plantier JL, Rival Y, Genoux Y, Lampugnani MG, Dejana E (1996) Thrombin-induced increase in endothelial permeability is associated with changes in cell-to-cell junction organization. Arterioscler Thromb Vasc Biol 16:488–496
Rappitsch G, Perktold K, Pernkopf E (1997) Numerical modelling of shear-dependent mass transfer in large arteries. Int J Numer Methods Fluids 25:847–857
Reed RK, Rubin K (2010) Transcapillary exchange: role and importance of the interstitial fluid pressure and the extracellular matrix. Cardiovasc Res 87:211–217

Ryan JW, Ryan US, Schultz DR, Whitaker C, Chung A (1975) Subcellular localization of pulmonary angiotensin-converting enzyme (kininase II). Biochem J 146:497–499

Schmid-Schönbein GW (2012) The integrin-cortex complex under control of GPCRs. Cardiovasc Res 96:7–8

Shen Q, Rigor RR, Pivetti CD, Wu MH, Yuan SY (2010) Myosin light chain kinase in microvascular endothelial barrier function. Cardiovasc Res 87:272–280

Shepro D, Morel NM (1993) Pericyte physiology. FASEB J 7:1031–1038

Spindler V, Schlegel N, Waschke J (2010) Role of GTPases in control of microvascular permeability. Cardiovasc Res 87:243–253

Sriram K, Salazar Vázquez BY, Tsai AG, Cabrales P, Intaglietta M, Tartakovsky DM (2012) Autoregulation and mechanotransduction control the arteriolar response to small changes in hematocrit. Am J Physiol Heart Circ Physiol 303:H1096–H1106

Stangeby DK, Ethier CR (2002) Computational analysis of coupled blood-wall arterial LDL transport. J Biomech Eng 124:1–8

Storch U, Schnitzler MM, Gudermann T (2012) G protein-mediated stretch reception. Am J Physiol Heart Circ Physiol 302:H1241–H1249

Sun Z, Martinez-Lemus LA, Trache A, Trzeciakowski JP, Davis GE, Pohl U, Meininger GA (2005) Mechanical properties of the interaction between fibronectin and α5 β1-integrin on vascular smooth muscle cells studied using atomic force microscopy. Am J Physiol Heart Circ Physiol 289:H2526–H2535

Sun C, Wu MH, Guo M, Day ML, Lee ES, Yuan SY (2010) ADAM15 regulates endothelial permeability and neutrophil migration via Src/ERK1/2 signalling. Cardiovasc Res 87:348–355

Tarbell JM (2003) Mass transport in arteries and the localization of atherosclerosis. Annu Rev Biomed Eng 5:79–118

Tarbell JM (2010) Shear stress and the endothelial transport barrier. Cardiovasc Res 87:320–330

Tarbell JM, Demaio L, Zaw MM (1999) Effect of pressure on hydraulic conductivity of endothelial monolayers: role of endothelial cleft shear stress. J Appl Physiol 87:261–268

Taylor GI (1953) Dispersion of soluble matter in solvent flowing slowly through a tube. Proc R Soc Lond A Math Phys Sci 219:186–203

Taylor GI (1954) Conditions under which dispersion of a solute in a stream of solvent can be used to measure molecular diffusion. Proc R Soc Lond A Math Phys Sci 225:473–477

Tedgui A, Lever MJ (1985) The interaction of convection and diffusion in the transport of 131I- albumin within the media of the rabbit thoracic aorta. Circ Res 57:856–863

Tsay R, Weinbaum S, Pfeffer R (1989) A new model for capillary filtration based on recent electron microscopic studies of endothelial junctions. Chem Eng Commun 82:67–102

Valvano JW, Bioheat transfer. users.ece.utexas.edu/~valvano/research/jwv.pdf

VanTeeffelen JWGE, Brands J, Vink H (2010) Agonist-induced impairment of glycocalyx exclusion properties: contribution to coronary effects of adenosine. Cardiovasc Res 87:311–319

Wagner WW, Latham LP (1975) Pulmonary capillary recruitment during airway hypoxia in the dog. J Appl Physiol 39:900–905

Wang DM, Tarbell JM (1995) Modeling interstitial flow in an artery wall allows estimation of wall shear stress on smooth muscle cells. J Biomech Eng 117:358–363

Weinbaum S, Curry FE (1995) Modelling the structural pathways for transcapillary exchange. Symp Soc Exp Biol 49:323–345

Werner J, Brinck H (2001) A three-dimensional vascular model and its application to the determination of the spatial variations in the arterial, venous, and tissue temperature distribution. In: Leondes C (ed) Biofluid methods in vascular and pulmonary systems. CRC Press, Boca Raton

Wissler EH (1998) Pennes' 1948 paper revisited. J Appl Physiol 85:35–41

Yeon DS, Kim JS, Ahn DS, Kwon SC, Kang BS, Morgan KG, Lee YH (2002) Role of protein kinase C- or RhoA-induced Ca^{2+} sensitization in stretch-induced myogenic tone. Cardiovasc Res 53:431–438

Zaugg M, Schaub MC (2004) Cellular mechanisms in sympatho-modulation of the heart. Br J Anaesth 93:34–52

Zhou X, He P (2010) Endothelial [Ca2+]i and caveolin-1 antagonistically regulate eNOS activity and microvessel permeability in rat venules. Cardiovasc Res 87:340–347

Zou H, Ratz PH, Hill MA (2000) Temporal aspects of Ca^{2+} and myosin phosphorylation during myogenic and norepinephrine-induced arteriolar constriction. J Vasc Res 37:556–567

Zou Y, Akazawa H, Qin Y, Sano M, Takano H, Minamino T, Makita N, Iwanaga K, Zhu W, Kudoh S, Toko H, Tamura K, Kihara M, Nagai T, Fukamizu A, Umemura S, Iiri T, Fujita T, Komuro I (2004) Mechanical stress activates angiotensin II type 1 receptor without the involvement of angiotensin II. Nat Cell Biol 6:499–506

Zunino P (2004) Multidimensional pharmacokinetic models applied to the design of drug eluting stents. Cardiovasc Eng 4:181–191